2012-04-20

Impact of Accelerometry and Spirography Data Analysis of Essential Tremor on BOLD-fMRI Data Interpretation

Saman Sargolzaei
University of Miami, s.sargolzaei@umiami.edu

UNIVERSITY OF MIAMI

IMPACT OF ACCELEROMETRY AND SPIROGRAPHY DATA ANALYSIS OF ESSENTIAL TREMOR ON BOLD-FMRI DATA INTERPRETATION

By

Saman Sargolzaei

A THESIS

Submitted to the Faculty
of the University of Miami
in partial fulfillment of the requirements for
the degree of Master of Science

Coral Gables, Florida

May 2012

UNIVERSITY OF MIAMI

A thesis submitted in partial fulfillment of
the requirements for the degree of
Master of Science

IMPACT OF ACCELEROMETRY AND SPIROGRAPHY DATA ANALYSIS OF ESSENTIAL TREMOR ON BOLD-FMRI DATA INTERPRETATION

Saman Sargolzaei

Approved:

_____ Mohamed Abdel-Mottaleb, Ph.D. Professor of Electrical and Computer Engineering	_____ Terri A. Scandura, Ph.D. Dean of the Graduate School
_____ Fatta Basil Nahab, M.D. Assistant Professor of Neurology	_____ Saman Aliari Zonouz, Ph.D. Assistant Professor of Electrical and Computer Engineering

SAMAN SARGOLZAEI (M.S., Electrical and Computer Engineering)
Impact of Accelerometry and Spirography Data Analysis (May 2012)
of Essential Tremor on BOLD-fMRI Data Interpretation

Abstract of a thesis at the University of Miami.

Thesis supervised by Dr. Akmal Younis and Dr. Fatta Basil Nahab.
No. of pages in text. (65)

Essential Tremor (ET) is the most common neurological movement disorder, with slowly progressive symptoms that impact the patient's quality of life and ability to perform activities of daily living. Tremors in ET occur during kinetic, with two subtypes: postural tremors and kinetic tremors. Postural tremors appear when the arms are topically maintained in a position against gravity, whereas kinetic tremors appear during sustained voluntary movements such as writing or drawing. The underlying mechanisms of either tremor type are not known, and further work is needed to determine whether they are two manifestations of the same brain dysfunction, or consequences of different underlying causes. To further understand these disease manifestations, we employed functional magnetic resonance imaging (fMRI) in conjunction with quantitative tremor measures (accelerometry and spirography).

Dedicated to my parents for their forever support; to love and patience my Mom gave me and to my dad who is the best teacher of my life.

Also to my friend and brother (arman) for being with me to overcome dificulties.

Acknowledgement

I would like to first give my great appreciation to Dr. Akmal Younis who is not among us today. Although I worked under his supervision for a short time and could not graduate with the Ph.D. degree, he taught me how to have a scientific problem-solving mind which was what I needed at the time. God bless his soul.

I would like to thank Dr. Fatta Nahab who introduced me to the beautiful word of functional MRI. He kindly found the unimproved parts of my academic and personal characteristics and in a friendly manner guided me to this point in my academic development. Working with him has effectively changed my career experience.

I would also like to thank Dr. Ishwar Sethi and Dr. Nilesh Patel who supervised me during my time with the Department of Computer Science and Informatics at Oakland University. They provided me with the first chance to study abroad and when I decided to transfer to the University of Miami they kindly wished me success. I hope I have the opportunity to work and learn from them again.

I am honored that Dr. Mohamed Abdel-Mottaleb and Dr. Saman Zonouz served on my committee. Their unbelievable support helped me overcome difficulties encountered along the way.

I am grateful to Dr. Kamal Premaratne for his wonderful help after the loss of my supervisor and to all the other faculty members who have taught me over the years.

Finally, very special thanks to all my friends who are the best. I count on your continued support from here on.

TABLE OF CONTENTS

LIST OF FIGURES

LIST OF TABLES

LIST OF ABBREVIATIONS

ACC	Accelerometry
BOLD	Blood Oxygenation Level Dependent
CSF	Cerebrospinal Fluid
DBS	Deep Brain Stimulation
EEG	Electroencephalography
EMG	Electromyography
EPI	Echo Planar Imaging
ET	Essential Tremor
FIND	Functional Imaging of Neurodegenerative Disorders Laboratory
FIR	Finite Impulse Response
FLAIR	Fluid-Attenuated Inversion Recovery
fMRI	Functional Magnetic Resonance Imaging
FOV	Field of view
FWHM	Full Width Half Maximum
GLM	General Linear Model
HRF	Hemodynamic Response Function
LAN	Left Anterior Nucleus
LBA17	Left Brodmann Area 17
LBA3	Left Brodmann Area 3
LBA4	Left Brodmann Area 4
LBA44	Left Brodmann Area 44
LCG	Left Cingulate Gyrus
LCOV	Left Culmen of Vermis
LCT	Left Cerebral Tonsil
LCUL	Left Culmen
LCUN	Left Cuneus
LDEN	Left Dentate
LDOV	Left Declive of Vermis
LFUG	Left Fusifoprm Gyrus
LINS	Left Insula
LIPL	Left Inferior Parietal Lobule
LLG	Left Lingual Gyrus
LMEDN	Left Medial Dorsal Nucleus
LMEFG	Left Medial Frontal Gyrus
LPACL	Left Paracentral Lobule
LPRE	Left Precuneus
LPUT	Left Putamen
LPOCG	Left Postcentral Gyrus
LPRCG	Left Precentral Gyrus
LRN	Left Red Nucleus
LSPL	Left Superior Parietal Lobule
LSTG	Left Superior Temporal Gyrus
LTHA	Left Thalamus
MABO	Mammiliary Body

MPRAGE	Magnetization Prepared Gradient Echo
MRI	Magnetic Resonance Imaging
OLI	Olive
PD	Parkinson Disease
PET	Positron Emission Tomography
RBA17	Right Brodmann Area 17
RBA3	Right Brodmann Area 3
RBA4	Right Brodmann Area 4
RBA6	Right Brodmann Area 6
RBS	Right Brain Stem
RCLA	Right Claustrum
RCT	Right Cerebral Tonsil
RCUL	Right Culmen
RCUN	Right Cuneus
RDEC	Right Declive
RDEN	Right Dentate
RF	Radio Frequency
RIOG	Right Inferior Occipital Gyrus
RIPL	Right Inferior Parietal Lobule
RLG	Right Lingual Gyrus
RMEDN	Right Medial Dorsal Nucleus
RMEFG	Right Medial Frontal Gyrus
RMIFG	Right Middle Frontal Gyrus
ROI	Region of Interest
RPACL	Right Paracentral Lobule
RPOCG	Right Postcentral Gyrus
RPRCG	Righ Precentral Gyrus
RPUT	Right Putamen
RRN	Right Red Nucleus
RSPL	Right Superior Parietal Lobule
RVLN	Right Ventral Lateral Nucleus
SEM	Structural Equation Modeling
SNR	Signal to Noise Ratio
SPM	Statistical Parametric Mapping
SPR	Spirography
TR	Repetition Time
VER	Vermis
Vim	Ventral intermediate

Chapter 1. Introduction to Essential Tremor

What is Essential Tremor?

Essential Tremor (ET), one of the most common forms of neurological diseases, along with Parkinson Disease (PD), Chorea, Tics and Dystonia are among the prevalent recognized movement disorders [Nahab et al. 2007]. While it is not a life threatening disease, Patients with Essential Tremor experience difficulties in their daily life due to the progressive behavior of essential tremor. 4% of people with the age over 40 years, increasing to 14% for people with the age of over 65 years, are suffering from Essential Tremor (ET) [Moghal et al. 1994]. Essential Tremor showed not to be gender dependent with a small more weight on male group [Nahab et al. 2007; Naqvi et al. 2011]. The "Tremor" is described by involuntary and rhythmic movements in one or more of body parts. Tremor could occur in parts of the body like arms, head, chin and soft palate with more likely to be observed in arms [Nahab et al. 2007]. While most of movement disorders occur in a mixed pattern, Essential Tremor (ET) is one of those which could occur almost purely in isolation. However depending on the state of disease by studying the syndromes, medical examinations and a survey of medical records, the correct diagnosis of the disorder to be able to treat it efficiently is a difficult task.

Essential Tremor (ET) is characterized by its non-jerky hyperkinetic syndromes in contrast with disorders characterized with jerky akinetic syndromes [Abdo et al. 2010] meaning that the oscillations follow a regular frequency varies between 4-12 Hz [Mansur et al. 2007], with varying amplitude depending on the disease stage (severity). Recording Electromyography and accelerometry are among the objective methodologies to quantify the rhythmic behavior of Tremor.

Genetic mutation has been found to be one of main reasons causing tremor, referred to as familial tremor [Deng et al. 2007], resulting in the need of family history of essential tremor in diagnosis stage. Exact causes of essential tremor are yet remained to be investigated but abnormal thalamic neuronal brain activities reported to correlate with essential tremor [Hua et al. 1998] in the deep brain. The Thalamus is specialized to function the coordinations and control the muscle activities in our body. From Consensus statement of the movement disorder society on Essential Tremor, Clinical diagnosis criteria for Essential Tremor are to be bilateral kinetic or postural tremor occurred largely on hands and forearms which is persistent, long term history of tremor, positive family history on essential tremor with the exclusion criteria of having other abnormal neurological signs [Deuschl 1998].

Primidone and Propranolol (first-line medications) and Acetazolamide, Alprazolam, Atenolol, Botulinum toxin, Clonazepam, Clozapine, Ethanol (to name a few from additional medications) are prescribed for the patients with Essential Tremor depending on their illness stage and diagnostic procedure for the past thirty years [Nahab et al. 2007; Louis 2012]. During the past few years, Deep Brain Stimulation (DBS) of Ventral intermediate (Vim) nucleus of the Thalamus [Kondziolka et al. 2008; Blomstedt et al. 2012] are chosen as the surgical treatment where the non-responsive pharmacological treatment is observed.

Choosing the right treatment from the huge diverse of agents and surgical treatments for each individual is essentially a complex formulation which cannot be granted successfully without having an accurate view of underlying mechanisms and pathways causing the essential tremor and observing the effects of the agents and various

treatments on individual subjects to have the power of statistically generalizing the effects to a population.

Essential Tremor and Different Modalities

Various pipelines with different modalities have been implemented to study the Essential Tremor and treatments where we briefly discuss electroencephalography (EEG), positron Emission Tomography (PET).

Parts of the brain are always communicating with each other even during rest periods. Communication signals are in the form of electrical impulses released from chemical processes in the background when a brain cell is functioning. Two types of EEG signals exist: One is the signal probed by the cortical surface electrodes placed on the scalp and the other uses special electrodes implanted inside the brain through a surgery to record intracranial EEG. Voltage differences between electrodes are measured and amplified and outputted as EEG signal. Using EEG technique, following electrical signal changes in the range of a few milliseconds is possible providing a high temporal accuracy in the recorded voltage potentials. One of the main clinical applications of EEG is diagnosing Epileptic seizure [Subasi et al. 2005] by characterizing brief and episodic neuronal discharges along with high amplitude which could be locally (partial seizure) or globally (generalized seizure).

Electroencephalography has been usually employed in conjunction with other modalities to study the essential tremor. [Hellwig et al. 2001] reported that activities in correlation with Essential Tremor could be detected on EEG whereas Magneto encephalography (MEG) failed to reveal cortical involvement in generation of Essential Tremor while it is theoretically expected that cortical involvement has correlation with the essential tremor

oscillatory since Thalamus, known to be the key point of Tremor generation, is a part of cortical network. EEG and EMG have been joined together to investigate whether the tremor in right and left sides have independent central oscillators [Hellwig et al. 2003] and it turned out while there is no complete independency but a dynamic synchronization exist among them. The drawback of Essential Tremor using EEG is that high temporal resolution of EEG recordings are yet not be able to overcome their spatial limitation.

Positron Emission Tomography (PET) is a three-dimensional imaging technique which is based on detecting pairs of gamma rays emitted from the subject tissue understudied. The pair of gamma photons is due to the annihilation between a positron, emitted from the deceleration of the radioisotope which was injected to the subject body, and an electron. The generated light is detected by a photomultiplier tube or a photodiode. PET imaging technique was employed in studying the neuroanatomical correlational activities corresponding to ET in cerebral cortex. It has been revealed by PET imaging on ET that we observe regional increase in cerebral blood flow in cerebellum, red nucleus, thalamus and primary sensorimotor cortex. [Boecker et al. 1996] investigate the ethanol responses for ET patients using PET technique and showed that ethanol has effects on decreasing the amplitude of the Tremor but keeps the frequency fixed.

Since the second chapter of the thesis has been devoted to the discussion on functional MRI, we here denotes briefly the idea of fMRI and postpone the comprehensive information on the subject to the next part. Functional Magnetic Resonance Imaging (FMRI) technique is an extension on Magnetic Resonance Imaging (MRI) to add the value of studying biological activities of the brain using magnetic resonance imaging techniques on top of investigating the brain anatomically. The importance of fMRI

observations due to its noninvasive and high resolution measurements from the brain organs under the millimeter scale has attracted enormous amount of attention to its opportunities and capabilities in the help of interpreting possible reasons of neurological disorders as well as the study of the new medications and analysis of treatments in addition to gain a more accurate comment on surgical risks. Analysis of functional connectivity of the of the brain with the aim of detecting the different brain networks and measuring the correlation between the fMRI time series, as a representative of how likely different parts in the brain are communicating with each other in response to a controlled stimulus, has been recognized as a helpful tool in the area.

It has been revealed that the changes in the level of oxygen consumption, which is roughly speaking what MRI measures, continues even in the absence of the controlled task where the researchers refer to it as resting state. Investigating the resting state networks (RSNs) which refers to find the regions with coherent fluctuations in the Blood Oxygenation Level Dependent (BOLD) signal is increasingly being deployed to study the movement disorders e.g. Essential Tremor. Functional Magnetic Resonance Imaging (FMRI) opened a new scientific window to study the essential tremor and its characteristics.

One main accurate finding that FMRI brought to is analyzing the cerebral activation pattern associated with essential tremor. In correspondence with one of the pioneer studies on activation pattern of essential tremor, the activation pattern included contralateral primary motor and primary sensory and the thalamus along with bilateral activation pattern of the nucleus dentatus, cerebellar hemispheres and red nucleus [Bucher SF et al. 1998]. One more interesting applications of Blood Oxygenation Level

Dependent (BOLD) Functional Magnetic Resonance Imaging (FMRI) is to allow surveying the functional connectivity of the cerebllar brain of ET. We went over Deep Brain Stimulation (DBS) of thalamus as a treatment for medication refractory in essential tremor. One challenge here is to precisely localize the thalamus considering the variability in individual anatomy. Functional connectivity aims at finding the brain networks responsible to direct an activity in the brain for a specific task. Finding the brain network involved in ET may decrease the variability in finding the thalamus in DBS surgery [Anderson JS et al. 2011].

Quantification of Essential Tremor

In order to quantifying the tremor, there have been three main methods proposed in the literature: Accelerometry, Electromyography (EMG), Spirogram, each with its own pros and cons.

Essential Tremor (ET) and Accelerometry (ACC)

One way to quantify and study the tremor is to use sensors to detect and record the acceleration. Accelerometer sensors measure the movements caused by the tremor. One thing about accelerometer sensors is the existence of gravity component in the measured signal. Gravity component gives the experimenter to identify the direction which has benefit in navigation applications. In most available laboratory measurements of hand tremor using accelerometry a three dimensional accelerometer sensor system is being hired. Among characteristics of the accelerometer system to be implemented for quantifying Essential Tremor are being capable to measure three mutual perpendicular axes acceleration, having a bandwidth with regards of frequency components of the tremor. Amplitude considerations are needed to be cared of. In some experimental

settings such as ours where functional MRI is being involved, Magnetic Resonance (MR) compatible setup is necessary. Figure 1-1 depicts a sample of recorded accelerometer sensors located to right and left hand (arm area) of a healthy person asked to simulate voluntary movements on his right hand. The first three axes are for the right hand and the second set belongs to left hand.

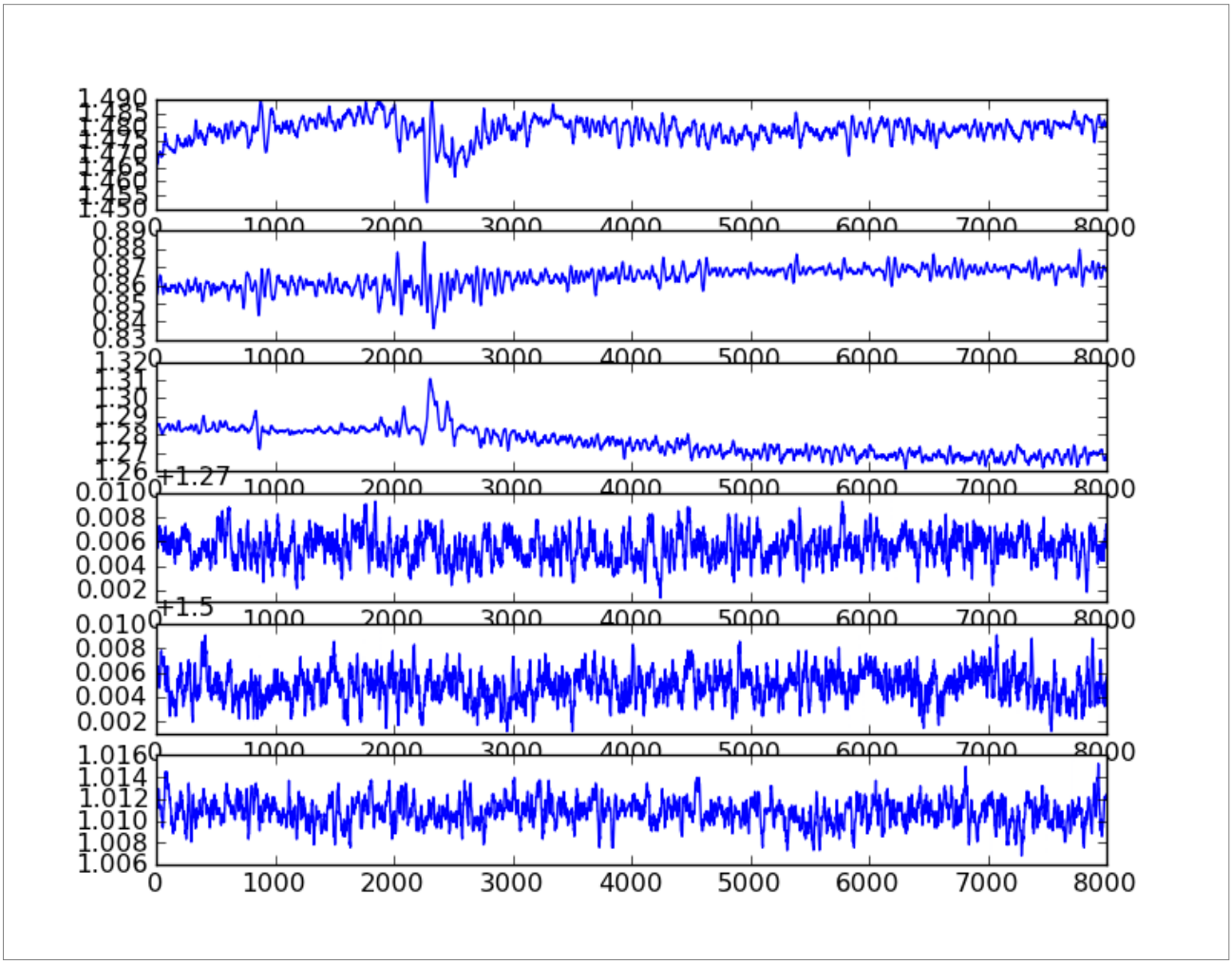

Figure 1-1: Acceleration recordings along three axes for right and left hands.

Essential Tremor (ET) and Electromyography (EMG)

Needle electrodes (invasive) and surface electrodes (non-invasive) are employed to record the electric discharging of motor units actively functioned in the pickup range. Electric discharging by a motor unit occurs when a muscle fiber is contracted due to

receiving an impulse from corresponding nerve. Depending on the strength of contraction and type of electrodes used for recording EMG signals as a superposition of motor unit action potentials (MUAP) have various rates of signal to noise. EMG is counted to be a way to quantify the tremor recent years. A raw EMG signal recorded using surface electrodes shows the motor units action potentials created due to contraction occurred during spasms on a leg muscle (Figure 1-2).

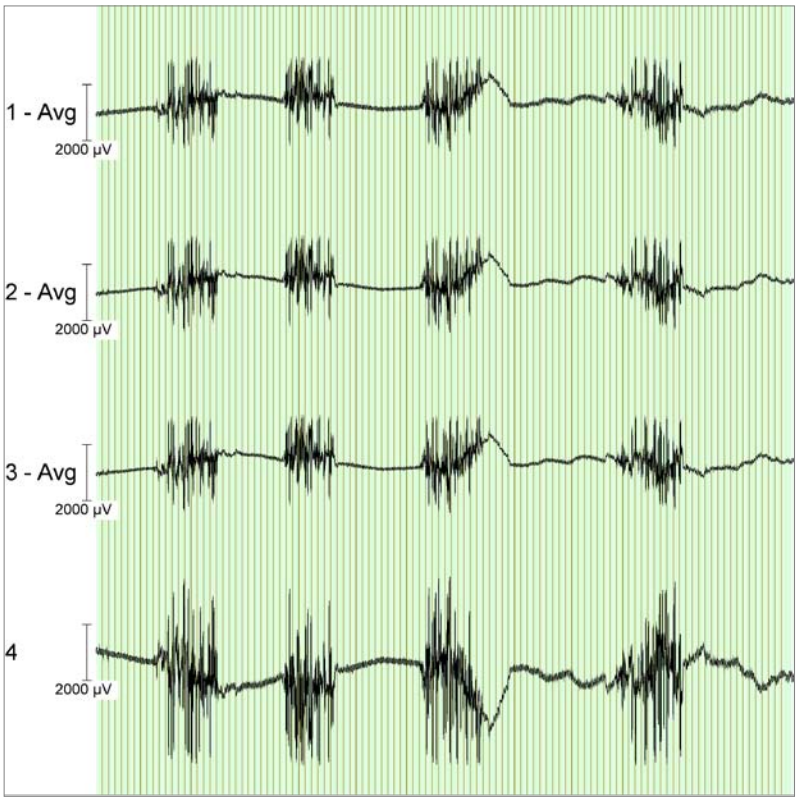

Figure 1-2: A sample surface EMG signal recorded during spasm generation.

Surface EMG signal passed through a de-noising process is recently used to command a robot developed with the aim of helping ET patients to perform daily activities with more convenient [Seki M et al. 2011]. One of the main challenges existed in current clinical diagnostic approaches are to determine the predominant type of movement disorder. One interesting study [Breit S et al. 2008] showed the efficiency of EMG in quantification and

differential diagnosis of pathological tremors. One of their findings is about the ability to differentiate between Parkinson's Disease (PD) and Essential Tremor (ET). As it is noted, one possible treatment for Essential Tremor is Deep Brain Stimulator where one or more electronic devices are implanted in Ventrointermediate of thalamus and tries to change the brain activity in a more controlled state. Wavelet and approximate entropy as a measure of uncertainty for the surface EMG signal are being proposed as a predictor of reappearance of essential tremor. While simplicity of EMG and being non-invasive technique to rely on in studies for Essential Tremor is clear but lack of spatial accuracy needs to be improved.

Essential Tremor (ET) and Spirography (SPR)

Circular and Squared spirals [Feys P et al. 2007] are among other ways introduced to quantify the tremor during which the patient is being asked to draw on a digitized tablet by the means of a special pen. The drawing action takes place two times, clock-wise and anti-clockwise directions. The positions where the pen and the surface touch each other are recorded. There is a standard spiral drawn on the tablet and patient being asked to draw following the background spiral on the surface. Analyzing the variations on the patient's drawn spiral from the standard spiral along two axes (x and y) could characterize the tremor. Squared and circular spiral methodology has been shown to be assessed for determining the severity of the intentional tremor which the regular clinical testing is the nose finger test [Feys P et al. 2007]. A sample recording of a circular spiral is figured in Figure 1-3.

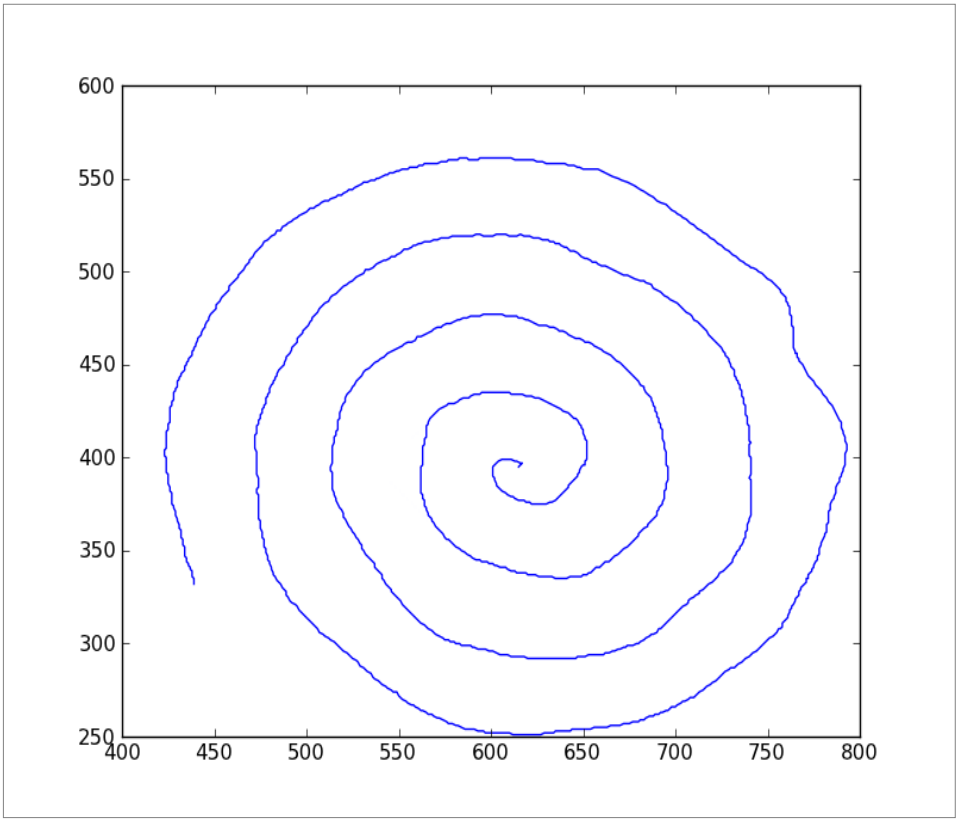

Figure 1-3: Circular Spiral drawn by a healthy person.

Thesis Goals

The main aim of the thesis is to provide a methodology to study and analyze ET in a multi-modalities environment (functional MRI and accelerometry, spirography). We aim to explore the brain regions involved in ET with developing a pipeline to generate the activation pattern, quantifying the tremor using quantifying data based on coherent analysis of functional magnetic resonance imaging (fMRI) experiment and two established measurement tools (Accelerometer and Digital Spirographam). For the purpose of this thesis, we report the results of our implementation on a dataset for a study conducted in the Laboratory for Functional Imaging of Neurodegenrative Disorders to investigate the causes of ET and the underlying mechanisms of treatment responses.

Thesis Database, Facilities and Experimental Setup

Database we are dealing with during this project is from an ongoing study directed by Functional Imaging of Neurodegenerative Disorders (FIND) Laboratory at Department of Neurology, University of Miami. The study is focused on exploring the mechanisms of Postural and Kinetic tremors in ET. Both these tremor types involve the arms while Postural tremor occurs when the patient is keeping the arms in gravity whereas kinetic tremor is observed during voluntary movements (e.g. drawing circular spiral). Two block tasks were conducted in this experiment and each block of task followed by a rest block. MR compatible setups for recording tremor (Accelerometer and Spirogram) were employed during the tasks.

During Postural task, Accelerometer sensors (two, one for each side) connected to the dorsum of each hand. The left side sensor is to monitor the subject movements during the rest block which should keep their arms at rest. The right side sensor is measuring the tremor when the subjects follow the presentation to do the posture task. Subjects were asked to elevate their right arm up to the middle point along the axis from the body to the MRI bore by hearting "posture" and maintain the posture situation for the whole block of task and return the arm to the rest situation by getting instructed to "rest". Recording of acceleration data were in synchronization with imaging the brain.

Kinetic task included fMRI experiment synchronized with recording on a digitized compatible MR tablet. During task block, subjects received auditory cue of "spiral" and "rest" to instruct them to start drawing the Archimedes spiral and put their arms at rest respectively. The tablet was located on their abdomen while they are inside the MRI bore and drawing of the spiral is followed by looking at a mirror reflecting the tablet surface.

Exact parameters for the fMRI, Accelerometer and Spirogram will be provided in the corresponding chapters of the thesis. Subjects underwent training before the scan starts to fulfill the requirements of the study.

As part of the ongoing study, All the experiments were repeated in two conditions to study the effect of Ethanol (EtOH) (plus propranolol are the two available and effective agents) on Tremor suppression and activation pattern on the brain. All data were prefixed with a "pre" to symbolize the data acquirement before taking the medication and "post" to count for data recorded after having the 50-ml dose of EtOh taken.

The processing pipeline of fMRI, Accelerometer and Spirogram were all conducted in our Linux workstation at FIND laboratory (8 Intel Xeon(R) CPU E5420 @ 2.50GHz cores, 15.8 GiB memory, 1.5 TB disk). Three publicly available software packages (AFNI, FreeSurfer, FSL) and libraries were mainly employed to process fMRI data (packages are implemented in order to satisfy our requirements). AFNI (might be an acronym for Analysis of Functional NeuroImages) is a set of freely available set of C programs for analysis and presentation of Functional MRI data developed initially at Medical College of Wisconsin and currently manipulated and maintained by a team at Scientific and Statistical Computing core of National Institute of Health [Cox RW 1996; Cox RW 2011]. The author of the thesis is honored to attend the AFNI training boot camp hold by the developer team on September 2009. We employ AFNI to implement our pre-processing stream and to generate statistical activation maps.

FreeSurfer is a set of publicly available automated tools developed at Martinos Center for Biomedical Imaging to reconstruct Brain's cortical surfaces from the anatomical data acquired during a functional MRI session [Dale AM et al. 1999; Fischl B et al. 1999].

Representation of cortical surface, pial surface, cerebellar segmentation of white matter (WM) and Cerebrospinal Fluid (CSF), Skull stripping are a few among the many abilities FreeSurfer provides. FreeSurfer serves in part to give us the the cerebellar segmentation for white matter and Cerebrospinal fluid mask and further to create Region of Interest (ROI) for the analysis.

Accelerometery and Spirography data processing pipeline is directed using a piece of software written in Python programming language developed by the author of the thesis. The codes are available by contacting the FIND laboratory.

The remaining chapters of the thesis are organized as follow: Next chapter is discussing the details on functional MRI, technical details on Image acquirement parameters, step-by-step preprocessing of functional MRI and our implementation of fMRI data recorded during the experiment, generating statistical activation maps in individual subject and group. The third chapter is specialized to quantifying the tremor in our sample; discuss the hardware to record the accelerometry and spirography; processing and characterizing the data; Time, Frequency analysis of objective quantification measurement of Tremor. Chapter 4 addresses the analysis of group functional MRI, Accelerometry and Spirography data in conjunction to explore the effects and provide a model to predict tremor severity using fMRI measurements. We are concluding the thesis on chapter 5 with report findings and suggestions for future work.

Chapter 2. Functional MRI Data Analysis of Essential Tremor

Entering to the fifth decade of Functional Magnetic Resonance Imaging (fMRI) studies and use of Blood Oxygenation Level Dependent (BOLD) contrast signal, there are still unknown facts being remained to uncover about this response and its physiological relation to activity of the brain. However following the undergoing investigations, most of the measured signal during the scan has its source in the nucleus (a dense region at the center of atom surrounding proton with positive charge and neutron with no electric charge) of the hydrogen atom (Nucleus has only one proton and no neutron for hydrogen atom) in the brain (While MR equipment being employed to different parts of body but we devote our attention only to the brain since now).

Human brain is a rich resource of hydrogen atoms considering the following statistics on how much of each includes water molecule H_2O (made from two hydrogen atoms and one oxygen atom): Blood with 93%, gray matter with 70% and white matter including 85%. These hydrogen atoms inside the water molecule are always rotating. Each atom may have different direction for their spin axis and consequently different rotational axis. Their spinning (rotation) is analogy to the rotation of the earth around the axis connecting the North Pole to the South Pole! In physics, net magnetic moment is referred to the spinning proton atoms considering their positive electric charge. Net magnetization of the proton atoms is zero due to the random momentum direction of each atom.

Inside the scan room of MRI centers, there is a magnetic field B_0 with strength of a few Tesla (T). The direction of the magnetic field is from feet to head of the subject while lying on the patient table inside the bore. Human medical imaging has reports in the range of 0.05 T to 8 T [Schenck JF 2000]. Going back to our analogy, we are

consistently surrounded by the earth magnet field with the strength of $5\times10^{-4}T$. It is clear how safety issues are to be kept about having a ferromagnetic object inside the MR room. The most out cylindrical part of the hardware is called Gradient and its job is to generate the magnetic field. Hydrogen atoms once they are located inside this magnetic field starts being aligned (in direction or anti direction) to the magnetic field direction but this alignment is not perfectly in line, instead, there is an axis change from the straight line in which the protons spin around their main axis. In fact all the protons spin around their new precessed axis with a same frequency called Larmor frequency and it is related to the power of the magnetic field by the following equation:

$$f=\frac{\gamma B_0}{2\pi} \tag{2-1}$$

Where γ is the gyromagnetic ratio (ratio of dipole mementum of an atom to an angular momentum) of hydrogen atom which is around 42.57 MHz/T. Frequency is also called resonance frequency. Resonance frequency in physics is referred to the frequency at which a system starts to oscillate in large amplitudes with an excitation. The mentioned excitation is produced in the MR equipment by Radio Frequency (RF) transmitters (one part of the RF coils) which excites the hydrogen atoms while they are spinning at their Larmor frequency inside the Gradient. The named wave transmitters are not always on unlike the Gradient which is always on. RF receivers absorb the released energy from the hydrogens when the transmitter is off. The latter process of excitation of a hydrogen atoms and receiving the released energy is the basis of acquired signal. It is worth to mention here that the power of looking at a particular group of hydrogen atoms localized at a specified place is directed by the gradient coils which give us the spatial resolution in an MRI session. In simple words, The key point in MRI is the varying signal emitted

from hydrogen nuclei in strength depending on the surrounding tissue. This is caused to have contrast in differentiating between Gray matter, White matter and cerebrosinal fluid in an image from the brain [Logothetis NK 2002].

Functional MRI (fMRI) is about how to put the contrast on the neural activity inside the brain. fMRI provides us such a measurement by discovering an interesting property of the Haemoglobin (delivers oxygen to neurons in the formd of capillary red blood cells). Haemoglobin shows diamagnetic features when oxygenated and paramagnetic when deoxygenated. Neural activity occurs in simultaneous with increasing in demand of oxygen which is delivered by Haemoglobin. By catching the changing record of blood oxygenation using MR signal, one can follow the neural activity occurrence in the brain. This MR signal recorded on changes on Blood oxygenation is called Blood Oxygenation Level Dependent (BOLD) signal. One more term is of interest to refer to here is Haemodynamic response which stands for the dynamic behavior observed in regulating the blood flow in the brain to maintain activities in the brain. By having considered this knowledge of fMRI, now let us take a look at some terminologies of MR:

MRI scan: A noninvasive three dimensional imaging technique using magnetic resonance phenomenon to create pictures of an area in the body.

fMRI scan: A form of magnetic resonance imaging of the brain with recording the blood flow to the active areas.

MRI Sequence: A special collection of radio frequency (RF) pulses and gradients settings to put contrast on a particular tissue signal aiming limiting the artifacts.

Localizer Sequence: A sequence involving low-resolution template images to place the slices in right position in 3-planes.

Axial Plane: An imaging plane bisecting the body into top and bottom parts.

Sagittal Plane: An imaging plane bisecting the body into right and left parts.

Coronal Plane: An imaging plane bisecting the body into front and back parts.

Fluid-Attenuated Inversion Recovery (FLAIR): A sequence to remove the effects of fluid (e.g CSF) from acquired images, applicable by having long T1.

T1 Relaxation time: A biological parameter which is a constant for each tissue type and is the time required for a tissue type to emit release the energy and realign with the external magnetic field.

Magnetization Prepared Gradient Echo (MPRAGE): A fast 3D acquisition with T1 weighted dominance.

Echo Planar Imaging (EPI): One of the first invented MRI sequences in which a complete image is formed from a single data sample (all k-space lines in one TR).

K-space: A space in which an image represented as a function of time and phase. Taking the Fourier Transform of an image in k-space leads to a MRI image.

Repetition Time (TR): The time gap between exciting a same slice with the pulse sequence.

Pulse Sequence: series of RF pulses, magnetic field gradient excitations with the aim of producing a specific signal to characterize some properties of the spin system.

Field of View (FOV): The distance across an image. Greater field of view more tissue coverage but decrement in field homogeneity.

Slice Thickness: The thickness of an imaging slice.

Volume: A three-dimensional image of the brain.

Voxel: A single unit in volumetric imaging.

Interested reader is referred to [Ogawa S et al. 1990]. The dataset studied for the thesis is acquired with the following scan parameters and order of sequences: 3-plane localizer, axial FLAIR, 3D T1 MPRAGE (1 mm^3 voxel), Axial EPI with contrast on BOLD (FOV: 24cm, Isometric voxels of 27 mm^3, TR of 2 seconds). 3 Tesla SEIMENS MAGNETOM Trio scanner is being employed to acquire images. The scanner reconstructs the images from k-space and save them in DICOM (Digital Imaging and Communication in Medicine) format with extensions of .dcm or .ima (SEIMENS) which each file is a two dimensional image. Our very first step in our pipeline for processing fMRI data is to convert the 2 dimensional images to three dimensional volumes to manipulate in the proceeded blocks. We choose NifTI format (with .nii extension) for our outputted format which is consistent for most availble processing workstations in neuroimaging setup. First a single NifTI volume for each time point is generated through a procedure of putting slices in order depending on the a priori information having in hand (sequential order or interleaved order) and subsequently the individual volumes that producing times series will be concatenated to generate one four dimensional NifTI file. Details on the mentioned formats are beyond our topic and reader is referred to find more detail on [Whitcher B et al. 2011].

The fMRI data we are dealing with during this chapter is named and summarized on Table 2-1 (subject S01 is symbolically noted here; There are 5 subjects analyzed for the thesis purposes). We need to emphasize on resting-state fMRI data where subjects have their eyes closed but instructed to not to think about anything particular but being wakeful during the slices acquisition. Following our recent investigations on the subject,

we found open eyes with looking at a gray background provides a more sensible outcome.

Table 2-1: A sample of raw data names in NifTI format.

	kinetic (kinetic task)	*posture (postural task)*	*rest*	*mprage*
pre	S01_kinetic_pre.nii	S01_posture_pre.nii	S01_rest_pre.nii	S01_mpr.nii
post	S01_kinetic_post.nii	S01_posture_post.nii	S01_rest_post.nii	

To extract the required information to step into the processing level and generate the activation maps, we have to pre-process the data to correct for artifacts and noises. The choice of pre-processing pipeline mainly depends on the nature of experiment, setup, understanding the paradigm and required outputs. While there are standard pre-processing methodologies proposed in the literature [Nahab 2011; Saad 2006] but they need to be adapted with each experimental setup. For our scenario we proposed the following flowchart to process functiobnal MRI data for Essential Tremor (Figure 2-1).

Preprocessing of fMRI Data of Essential Tremor (ET)

Structural fMRI Data

Anatomical dataset which we name them here as structural data is processed with three main goals: 1. To serve as an underlay for functional images, 2. To employ sub-cortical segmentation data to create masks of region of interest (ROI) for 2nd level analysis and 3. To prepare images for transferring to a standard space and group analysis. To aim these goals processing of structural dataset (T1-weighted e.g. S01_mpr.nii) is done using FreeSurfer. Figure 2-2 shows three views (axial, sagittal and coronal) of raw structural dataset.

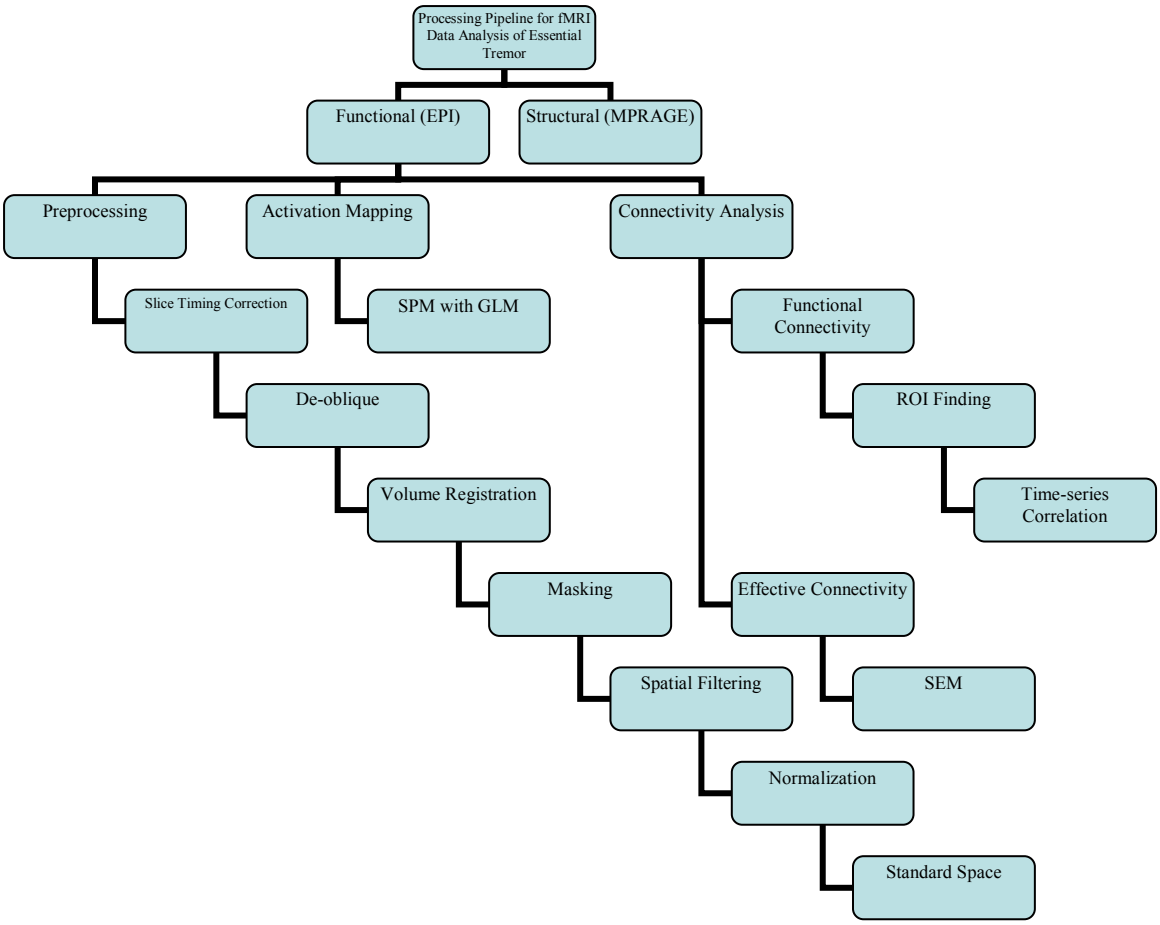

Figure 2-1: Proposed Pipeline for fMRI data analysis of Essential Tremor

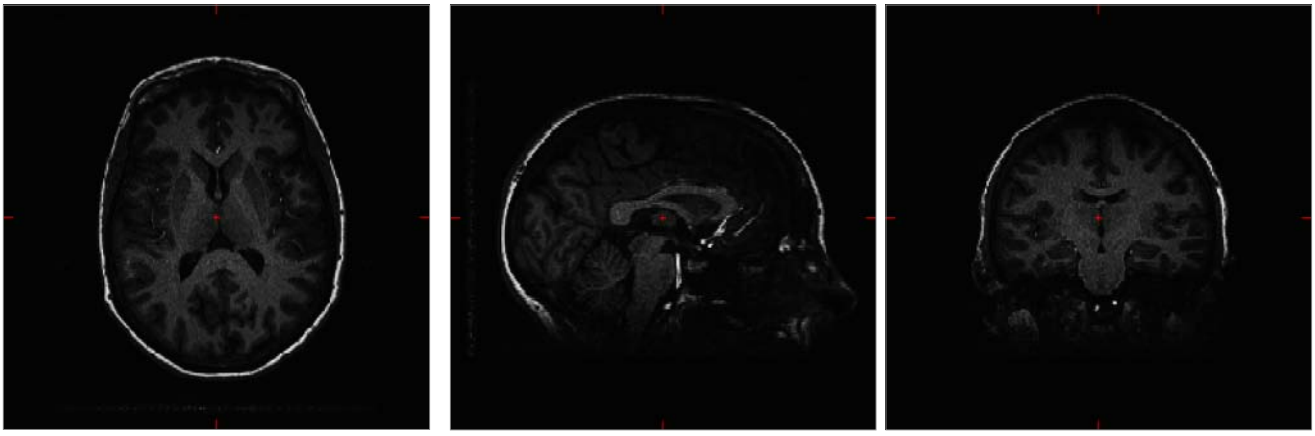

Figure 2-2: Axial, Sagittal and Coronal views of raw structural data for subject S01

The regular processing streamline of FreeSurfer reconstruction (reconn-all script automatically does the process as desired) includes following with having in mind that

not all of the steps were applicable to our datasets and dataset needs to be converted to a format recognizable by FreeSurfer (.mgz format):

Motion Correction

In case of acquiring more than one volumetric dataset, they are aligned spatially to the template volume (this could be one of the acquisitions) and their average is being computed and served as the input to the next step. Here we had only one set of structural data over individuals.

Intensity Adjustment, skull stripping and Talairach transformation

This step is first trying to correct for non-uniformity intensities along the volumetric dataset. This is done by histogram matching between each subject dataset intensity histogram and the FreeSurfer atlas image intensity histogram. The next job is to find an affine transformation from individual space to a standard space to prepare data for group analysis. Standard space here is chosen to be Talairach imaging space [Talairach J et al. 1988] which is a standard space in localizing brain organs independent from intra-subject variability. Before going to the standard space, a watershed algorithm [Segonne F et al. 2004] is being applied to the intensity normalized volume to remove the non-brain tissues e.g. scalp, skull, neck tissue, etc. Figure 2-3 is the output from the second step for the same subject. At this step, the care needs to be taken especially when you are involving with quality control to check the data visually and manually correct for the errors. Output of this step is being inputted to the Brain Extraction Tool (BET) [Smith SM 2002] to create a binary mask of the brain with functionality on functional fMRI data preprocessing which will be discussed next section. A sample of the generated binary

mask from BET overlaid on top of the anatomical image is described in Figure 2-4. Red areas are represented voxel values of 1's and other areas have 0's for the voxel values.

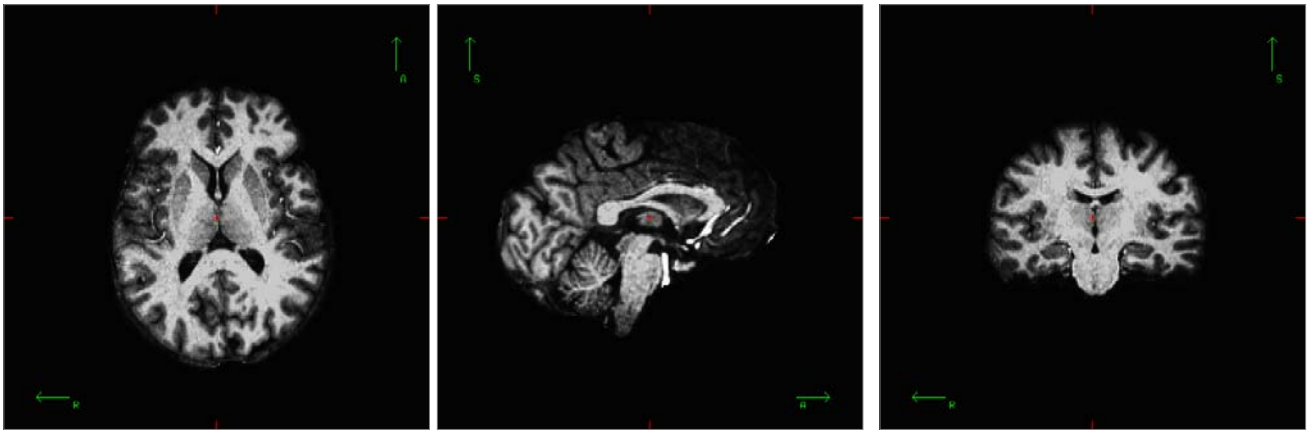

Figure 2-3: Intensity corrceted, non-brain removed, Talairached transformed structured data for subject S01.

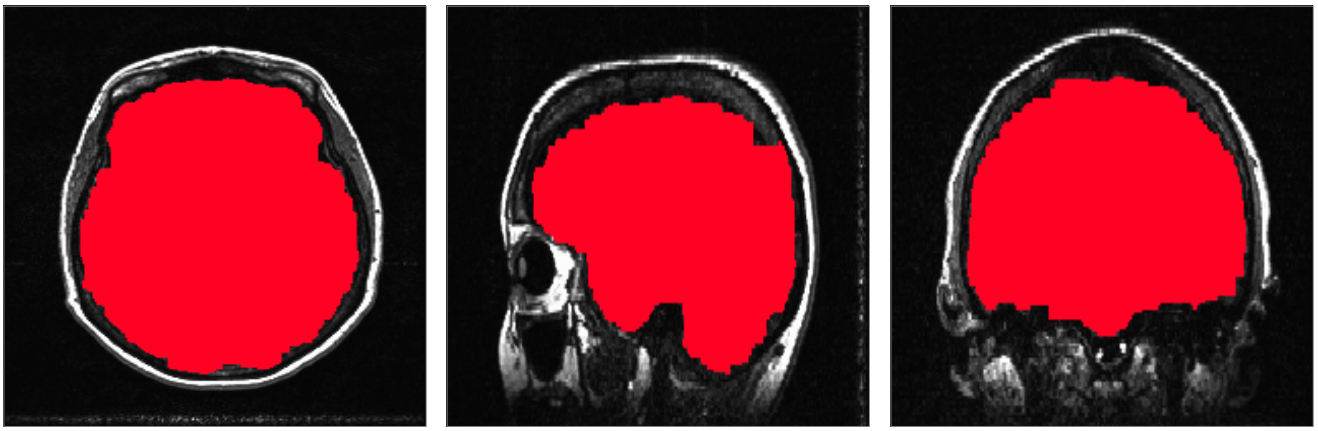

Figure 2-4: Brain mask extracted using FreeSurfer.

Sub-cortical Segmentation

At this step, FreeSurfer atlas brain image will be warped through a non-linear transformation to the subject brain atlas and labeling were proceeded by utilizing the warped atlas and different tissues (sub-cortical structures, brain stem, cerebellum and cerebral cortex) were labeled accordingly [Khan AR et al. 2008]. This stage takes the longest. Figure 2-5 is the output from the segmentation step. Output of this step is also of

importance since unbiased ROI masks could be created from the output of this segmentation procedure.

From this step ahead, hemisphere's cortical surface representation based on surface inflation, projection, topology correction and finally surface parcellation are not required in our pipeline and we do not cover them but they could be automatically generated by the script. Important statistics could be measured such as brain volume, surfaces area and measured cortical thickness.

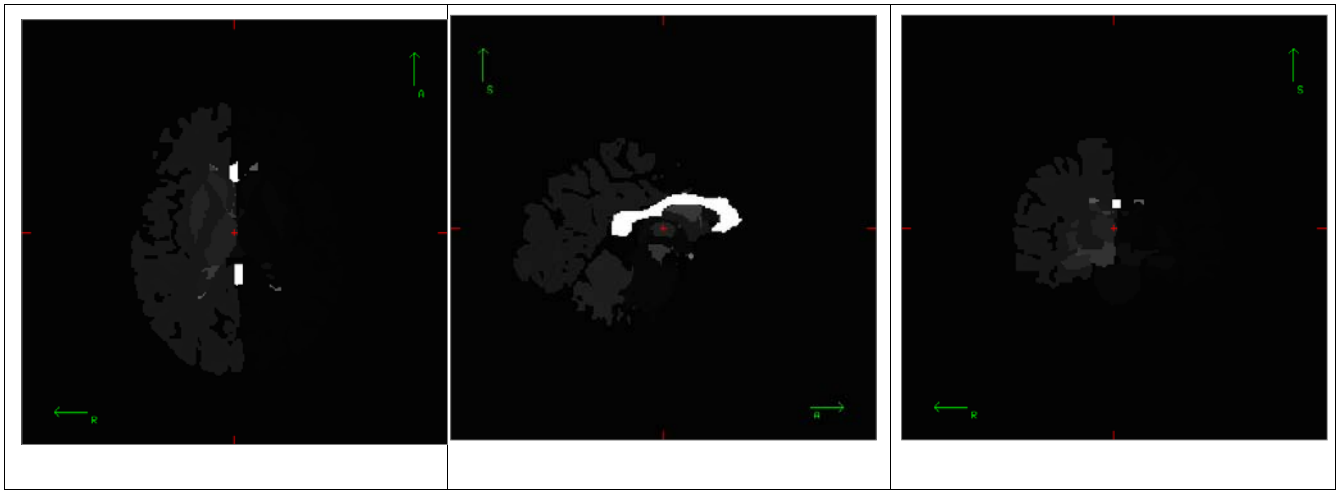

Figure 2-5: Sub-cortical segmentation of the brain for subject S01.

Individual functional data preprocessing

Main goal in preprocessing of functional MRI data is to correct for variabilities occurred due to non-task components and prepare data to extract the task related activities with higher signal to noise ratio using processing methodologies such as General Linear Model (GLM) and analysis of variances which are task corresponding. There are pipelines proposed to pre-process the fMRI data but it has not to be counted as a rule of thumb. Implementing a streamline for preprocessing and applying the GLM to detect the activity pattern requires the need of being aware of data acquisition procedure, nature of experiment, expected outcome. It is ideal for a person who processes the data to be

present during the experiment and visually record the session if applicable. The thesis author was not available when the current data were acquiring so tried the best to gather as much information to have a reliable picture of the data recording with the help of the PI. There are tools specialized for processing, statistical analysis and displaying brain imaging data in both clinical and research disciplines: AFNI, Brain Voyager, VoxBo, SPM. Once the scanning session starts, there is a time delay until the spin system of the MR acquisition reach to its steady state what is called equilibrium. During this time delay, RF receivers are not on and no signal is acquired while the scan is started. The mentioned scans are called dummy scans standing for non-informative character of them. It is interesting to know that the initial scans are in higher quality compared to the latter ones and in some ways; they could be effective when image registration is the quest. Some hardware equipment automatically gets rid of dummy scans. In case of not automatically removing them, the care needs to be taken. Here we explain our steps to process ET data with the underlying philosophy to choose a special methodology.

Slice Time Shifting (_ts)

The beauty of recent brain imaging technologies is to give the experimenter a nice shot of ongoing activities in the whole brain at a moment e.g. by employing fMRI , we are paying care to the recorded activities in BOLD signal in all parts of the brain at a same time. The current hardware limitation enforces us to acquire one image slice (axial) at a time. Therefore there is a time delay in slice acquirement when we move to next slice. Let us take a closer look at the subject. One needs approximately to acquire twenty slices with each slice having a thickness of about five millimeter to cover the entire brain [Boller F et al. 1994]. Assuming TR of two seconds implies 100 milliseconds of time lag

among measuring the changes in BOLD contrast fMRI signal for each upcoming slice. This shows the necessity of correcting especially in larger TRs.

Although the delay might seem a small number but considering the physiological changes e.g. changes in the BOLD signal, Changes in the heart rate, respiration, etc., the slices time series are required to be corrected to the same origin of time to have a statistically reliable map of how the brain areas respond to a stimulus simultaneously. Shifting operation of the slice timing is done by determining a time point as a reference. Reference could be the first time point of the first slice and then temporally shifting the time points of each slice with the value of the shift measured based on the order in which the slices are being scanned (ascending or descending) and also using the knowledge whether the data are scanned interleaved (The reason of interleaved scans has been mentioned to increase the Signal to Noise Ratio as the result of having the steady magnetization). The mentioned information could be extracted from the hardware manual. In fact by slice timing correction, we are trying to resample the data and find the equivalent MR signal value for the same time points as the time points for the reference slice (e.g. the first slice) and it is usually done by interpolating the samples at known time points to find the missing samples at given reference time points.

The interpolation could be done in different shapes: Interpolation using the Fourier transform which is finding the Fast Fourier Transform (FFT) of the MR signal and then shifting the phase of the signal by multiplying with an exponential component. The required information of the scanning order and the frequency of the scan could be retrieved from the header file of the dataset. Aliasing phenomenon has to be considered

since interpolation may affect the data components with having frequency components above the nyquist-shannon frequency.

Interpolation based on the Fourier Transform is the most accurate and slowest method. Other shapes of interpolation include linear interpolation which is the fastest one and at the same time it is suffering from the least accuracy, cubic interpolation using the 3rd Lagrange polynomial which is the conventional one, 5th order Lagrange based interpolation, etc. The smoothing effect of the linear interpolation is observable in using the first order Lagrange polynomials.

On the order of applying the timing shifting, there is a rule of thumb recommending shifting the slices time before correcting for the motion which is the next step for the data which has been acquired in an interleaved fashion. In sequential acquisition, slice timing correction is better to be taken after motion correction. In our implementation, we applied the time shifting based on the interleaved ascending slice acquirement using the cubic interpolation for creating the new time gridding.

De-obliquity correction (_do)

This step is more an optional to be a default step but is required to be included in our pipeline since in order to mask out the non-brain regions. We acquired our optimized brain mask from processing the structural data explained in previous part where we worked with anatomical dataset. Furthermore, A part of the dataset understudied here is acquired in oblique coordinate whereas the anatomical images were acquired in usual cardinal coordinate (There are some anatomical acquired in oblique space). If we do not correct for difference in cardinal and oblique coordinate for functional and structural, we will have distorted data in output by applying any spatial transformation on a dataset and

also during masking procedure. Transferring the coordinate causes blurring the data in according to the interpolation effect. It is not recommended to include this step where both structural and functional data are acquired in the same coordinate or the masking procedure is not based on structural such as in our case.

Volume Registration (_vr)

Gaining to an acceptable spatial resolution in addition to the temporal resolution is being mentioned as one power factor of fMRI in comparison with other imaging techniques to study the functionality of the brain. With the resolution of about 3 millimeter in plane, what will happen if there is a spatial displacement of the voxel position during the experiment as small as a few millimeter?! Although the subject is being asked not to move (Not surprisingly something unachievable at least because of respiration!) or try to minimize the movement during the experiment and also the head is being fixed in the scanner, however the slices are needed to be motion corrected. In our study, the case is more difficult since the motion is inseparable part of ET. It is worth to note that one missing part we are observing in the traditional motion correction algorithms is not to count for the task-related motion effects and this is going to be one future direction of the author research direction. The other important potential here is the limitation of current techniques in correcting movements larger than a few millimeters.

Without considering the possible sources of motion such as movements caused by the nature of the task, motions due to the pulsation and respiration or other reasons, most of the existing methods for motion correction employ rigid body registration method in which the shape of the head is being assumed not to change during the whole scan (satisfying the rigidity property) and try to register with 6 degrees of freedom: three

translations (namely dx, dy, dz) and three rotations (Roll, Pitch, Yaw) each slice to a base slice to optimize (maximize or minimize) a cost function which could be the penalty function of least squares [Cox RW 1999] or Mutual information of consecutive slices [Kim B et al. 1999]. One of the main benefits of the registration is to have a measure of how reliable the statistical parametric mapping could be. Also motion parameters can be used as a feedback to the subject to increase the accuracy of the analysis in real time fMRI studies developed recently. Head motion is done on individual basis for each run separately. For our implementation, we consider the first brick (Image slice) of "kinetic_pre" dataset (first run) as the reference image to align the subsequent images as well as other datasets to. The choice of reference is subjective while we choose the first slice of the first run as the reference image with the assumption of having the less motion for the first time points of the first run. Table 2-2 provides detail information about maximum displacement for each subject per run. Figure 2-6 and 2-7 shows the estimated motion parameters and its derivative for first subject. The subplots describes six estimated movements: rotation about the Inferior-Superior axis, rotation about the Right-Left axis, rotation about the Anterior-Posterior axis, displacement in Superior direction, displacement in Left direction, displacement in posterior direction. High correlation between the paradigm template and movements during each run (150 time points) is clearly observable. To reduce the effect of this confound on activation maps, derivative components are employed for GLM.

Masking

Explained before, a brain mask needs to be created and applied on the functional data to remove artifacts which are referred to as susceptibility artifacts and occurs on the

boundaries. Susceptibility artifacts are results of non-homogeneous character of the magnetic field. One option is to create a mask from the EPI data whereas we employed FreeSurfer anatomical brain extracted mask due to its higher accuracy in covering the brain regions and excluding non-brain tissues and air resulting in accurate signal intensity.

Table 2-2: Maximum displacement for each subject per run and the corresponding sub-brick

	kinetic_pre	**rest_pre**	**posture_pre**	**kinetic_post**	**rest_post**	**posture_post**
S01	1.14 mm (139)	1.17 mm (146)	5.43 mm (11)	13.95 mm (9)	13.27 mm (148)	15.40 mm (139)
S02	4.52 mm (122)	2.80 mm (121)	5.68 mm (139)	8.25 mm (139)	8.25 mm (121)	6.25 mm (142)
S03	4.91 mm (121)	7.95 mm (11)	10.35 mm (134)	16.21 mm (89)	15.29 mm (3)	14.55 mm (15)
S04	3.02 mm (98)	2.30 mm (1)	4.14 mm (100)	10.26 mm (60)	7.90 mm (148)	8.13 mm (43)
S05	4.27 mm (117)	1.98 mm (148)	2.96 mm (138)	10.49 mm (136)	8.52 mm (145)	7.94 mm (19)
Mean	3.57 mm	3.24 mm	5.71 mm	11.83 mm	10.64 mm	10.45 mm
SD	1.53 mm	2.69 mm	2.81 mm	3.19 mm	3.4 mm	4.2 mm

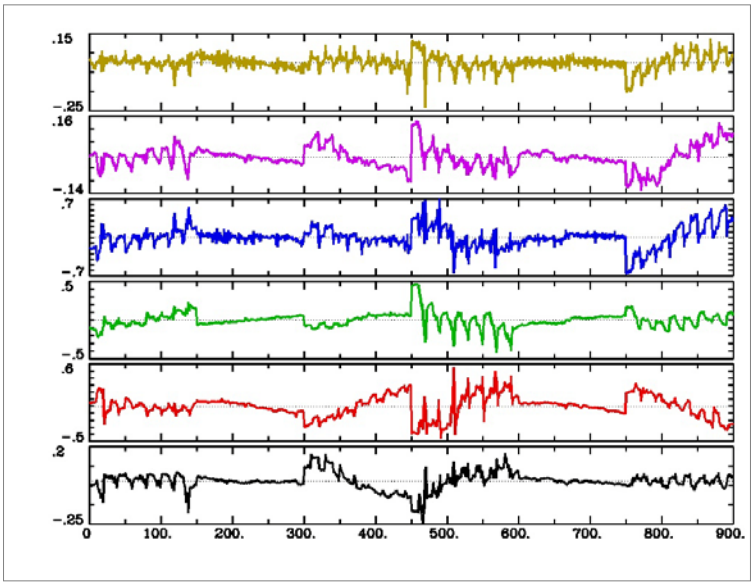

Figure 2-6: Estimated motion parameters in volume registration.

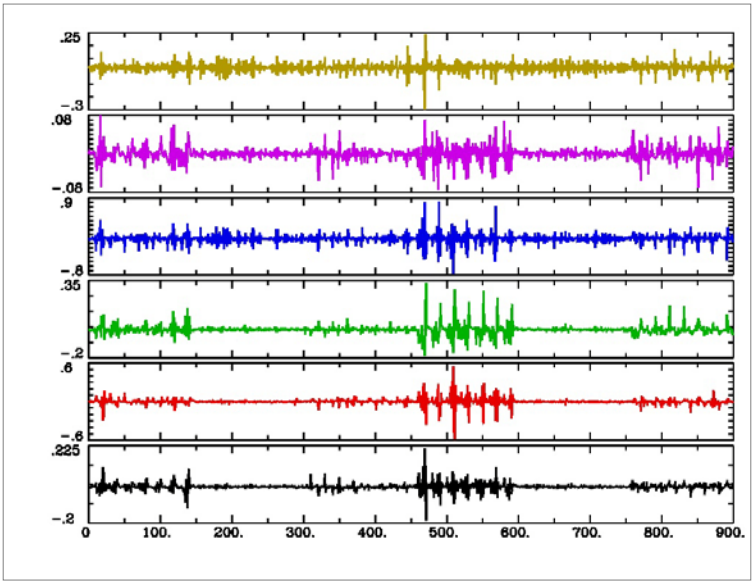

Figure 2-7: Derivative of each motion component estimated in volume registration.

Our generated FreeSurfer brain mask is required to be re-sampled from its fine grid (anatomical resolution) to the coarse grid resolution which is functional runs in our case. At this step, brain mask is re-gridded to match functional resolution and then multiplied by the volume registered images (_vr) to exclude non brain regions from our analysis.

Spatial Filtering (_blur)

By spatial filtering of fMRI data, we are trying to globally increase the signal of interest and at the same time reduce the effects of unwanted resources assumed to have a random occurrence nature. It has been shown that the high frequency components of the measured signal have fewer sources in the neural response of the brain and mostly they are coming from the sources. Then to increase the SNR, we are employing the low pass filtering in the spatial domain. Another interpretation of Increasing the SNR by averaging the measured signal in its neighbors comes from the fact that the response to a stimulus mainly extends over several voxels not a single voxel and in general the interested component of the signal comes from a normal distribution and matched filter theorem

could be another evidence of using the Gaussian kernel to blur the data and as result increase the SNR.

Improving SNR is not the only reason to apply a blurring function. Other factor is that by applying efficient smoothness, it is ensured that the discrete samples could be considered as a good representative if we were doing our analysis in continuous spatial space. Furthermore by smoothing the measurements we are moving one step forward to prepare the data for the group analysis due to the anatomical changes between the subjects. One of the conventional smoothing operators is mathematically being done by convolution between the 3D volume and a Gaussian kernel which is a bell shaped curve representing a normal distribution. The Gaussian distribution being defined by its mean and standard deviation from the statistical point of view as the following equation shows:

$$G_{1D}(x) = \frac{1}{\sqrt{2\pi\sigma^2}} e^{-\frac{(x-\mu)^2}{2\sigma^2}} \tag{2-2}$$

The above formula can be easily extended t N dimensions by simply replacing the x by a vector and put a power of N on the normalization factor. Standard deviation shows how the curve extends sharp the curve is. Another way of describing a Gaussian kernel especially when smoothing effect of the kernel is of interest could be by measuring the Full Width Half Maximum (FWHM) of the kernel and it is the width of the curve at its half of the maximum value. The relation between the standard deviation and FWHM is expressed in following equation:

$$FWHM = \sigma\sqrt{8\ln 2} \tag{2-3}$$

Therefore a Laplacian filter (Gaussian kernel) can be completely defined by its center and its FWHM and to apply the filter on the data, all we need is to consider the data values

located under the curve with the center at one of the delta values and multiply every data value by its equivalent kernel value and add them up together and finally divided by the normalization factor and replace the new value for the center of the data point placed under the center of the kernel.

The center is then being shifted successively to cover all the data points. It has been mathematically proven that to implement a multi dimensional Gaussian filtering one can apply 1D Gaussian kernel in N times orthogonal passes on the data. The mentioned method is also less computationally expensive due to the number of needed multiplications/ additions.

Considering the three dimensional Finite Impulse Response (FIR) filtering e.g. in a case of 3mm*3mm*3mm with a 6mm FWHM kernel, the value of the voxel under the center gains its weight by 50 percent from its own value and 50 percent from the 6 neighbors. Wider FWHM means more smoothness applied on the data. The value of x shows the distance from the center of the curve. In our experiment, the smoothing procedure continued to reach four millimeter in FWHM parameter locally and globally.

Normalization (_scl)

Scaling the BOLD response attempts to map every changes in the measured MR signal to a unique measurement space which is presenting the changes of the response of a physiologic unit(s) of the brain to a stimulus from the baseline (Rest) in percentage(s) and then by this normalization we can have a standard measure of how many percentage the signal changes from its mean value. The mentioned scaling helps us to study the responses intra subjects. The following numerical example shows the benefit of normalization in the fMRI study. Consider an experiment done on two subjects and by

looking at the time courses of each one of the subjects separately we see that for one of them the measured signal has been changed from 200 (the value of the baseline) to 220 (at the time of the brain's response to the task) and for the other subject the BOLD signal has been varied from the value of 734 (at baseline) to 807.4 (at stimulus condition). By first look and without any normalization the numbers say more changes in the second subject response change (73.4) than first subject response change (20) show more than twice activation in the second subject which is not a true conclusion.

In the latter example we disregard the fact that the baselines of the two signals are different from each other due to any differences from their biological perspective while in fMRI studies, percentage change from the baseline at the time of the stimulus being applied is important for us. Therefore one default step has been added to the preprocessing steps and during which the measured signal will be divided (There are different schemes for normalizing purposes) by its mean (baseline value) and multiplied by 100 to gain a standard measure what is called the percentage change of the signal. By applying this simple formula we see that both subjects in the latter example have a similar change of 10% in their response.

At this step, mean value of each time course corresponding to each voxel in the brain volume is computed and time course is normalized by the mean and the output is multiplied by hundred to have the percentage signal change.

Removing the trend (_dtr)

The aim of implementing this part of the pipeline is to remove the systematic incremental or decremental fashion observed in the in a fMRI signal. This trend is due to the physiological and instrumental noises surrounding signal. Since any statistical procedure

such as General Linear Model is based on finding changes with statistically significant changes from a base line, the trend needs to be removed from the fMRI signal before statistical inference. We considered second order Legendre polynomial to remove the trend in our implementation.

Spatial Normalization (+tlrc)

Considering the differences along subjects, for further exploration, they need to be studied at a standard space. Our default standard space is Talairach space. Recalling transformation we applied on the structural data to travel from original space to standard space, it is straight way to use the same transformation matrix to bring the functional dataset (+orig.) to the standard space (+tlrc.).

Our preprocessing pipeline is ended at this step. The resulted fMRI data is not ready to be studied statistically to create the activation pattern and compare the inter-subject map, extracting the average signal along subjects for regions of interest, implementing the correlation-based connectivity analysis. There are other available steps which could be considered depending on the experiment, such as temporal filtering of time courses to remove unwanted frequency components and needed a priori information to avoid distort signal of interest.

Functional MRI Based Activation Mapping

One main preliminary output reported in most of fMRI studies is the activation map of the experiment with statistical value added. General Linear Model (GLM) implemented by de-convolution procedure [Cox RW 1996] is a simple and most prevalent way of generating activity pattern in fMRI while author of thesis believes it could not be the

optimized solution in ET study due to some unsatisfied assumptions of GLM with de-convolution which will be discussed later. We implemented Ordinary Least Square Regression analysis though the de-convolution script provided by AFNI. fMRI time series at each voxel is considered as a linear combination of baseline parameters and the neurological activity of the brain. Baseline is a set of regressors of no interest (e.g. motion parameters). The neurological activity is modeled by a convolution operator between Hemodynamic Response Function (HRF) and the timing paradigm of the experiment (blocks of task followed by rest in block related experiment). Having an assumption on the shape of the HRF is one limiting factor on the model-based methods proposed for fMRI data analysis. Statistics are able to provide the experimenter with the significance level of a set of regressors against the full model. We briefly describe what GLM does in our implementation of ET fMRI data analysis [Friston KJ et al. 1995].

It is called General Linear Model since it aims in defining a general linear model for an underlined process. In our experiment, we define the observation time series as follow:

$$\begin{aligned} Y_1 &= X_{11}\beta_1 + X_{12}\beta_2 + \ldots + X_{1m}\beta_m + e_1 \\ Y_2 &= X_{21}\beta_1 + X_{22}\beta_2 + \ldots + X_{2m}\beta_m + e_2 \\ &\vdots \\ Y_p &= X_{p1}\beta_1 + X_{p2}\beta_2 + \ldots + X_{pm}\beta_m + e_p \end{aligned} \qquad (2\text{-}4)$$

In this representation of our acquired time series: Y_i with i varied from 1 to p are the measured fMRI signals (contrast on BOLD) and we referred to it as observation. X is called explanatory variable (elements of a matrix) which is given and β's are the unknown coefficient needed to be estimated. e is the residual error which could be drawn

from a normal distribution with a slight assumption on noise processes (Independent and Identically Distributed i.i.d). Putting them into a matrix from will yield into:

$$Y = X\beta + e \tag{2-5}$$

It is been explained in experiment presentation chapter that our experiment included four effects (kinetic_pre; posture_pre; kinetic_post; posture_post) pseudo randomly presented among blocks with rest condition presented with a "+". Columns of design matrix X correspond to each component which has a contribution into the observed variance and each row has a correspondence in estimated parameters (Either ideal time series or confounds such as motion parameters). Here is the point of ambiguity in GLM approach. Design matrix depends on the shape of HRF assumed for modeling the neural process due to the activity occurring in brain. In our implementation, HRF assumed to be of Mark Cohen's gamma-variate function which most likely present current understanding of BOLD signal changes in a volume of neuron's firing event. The function is convolved with stimulus paradigm and considered as known components in the design matric. Least squared approach to estimate β parameters is followed:

$$\beta = (X^T X)^{-1} X^T Y \tag{2-6}$$

To give statistical inference into the results GLM approach, the criterion is to use t-statistics. One tests the result against the Null hypothesis which assumes of non-existence of the current effect. In simple words, let us assume we considered estimation strategy for 4 parameters (four fixed effects which are our conditions during the experiment). We could define a contrast vector to test whether "kinetic_pre" has any difference statistically significant from "kinetic_post" against the Null hypothesis with no statistical significance:

$$C = [1 \quad 0 \quad -1 \quad 0] \tag{2-7}$$

T-statistics for this hypothesis is computed by:

$$T = \frac{c^T \beta}{\sqrt{\text{var}(c^T (X^T X)^{-1} c)}} \tag{2-8}$$

Two important considerations in our pipeline for ET fMRI data analysis are: 1. Concatenating runs to generate as more data points with the goal of increasing accuracy in computing the significance of our reported statistics (The concatenation order: kinetic_pre; posture_pre; rest_pre; kinetic_post; posture_post; rest_post); 2. Including the first derivative of the extracted motion parameters as regressors of no-interest in the model to increase sensitivity in the maps. The inclusion of motion parameters by their own had reported falsified pattern due to the task correlated pattern of the extracted motion. Statistical activity map for each run in individual subject basis has been computed using GLM de-convolution process.

Results of Statistical Activation Mapping

Individual subject maps underwent a two-factor analysis of variance (ANOVA) to create the group map for each condition. To cave into more detail on the experiment and processing result, we propose a guideline: creating the group activation map per condition, identifying the survived clusters from correcting p-value, going back to individual space and observing the percent signal change in an individual basis along with average fMRI BOLD signal for the center of survived clusters. Mixed effect model of Analysis of Variance (ANOVA) is being implemented. The group maps for each condition outputted from ANOVA has been corrected with p value of 0.05 clustered with minimum size of clusters to be 20 voxels. Figures 2-8 and 2-9 are the group maps after

correction for p-value of 0.05 and clustered for posture task and spiral task respectively. Tables 2-3, 2-4 includes the cluster information and atlas coordinates to be used in next level of processing when we go to individual subject activation maps. Cluster name abbreviations are given in abbreviation table of the thesis.

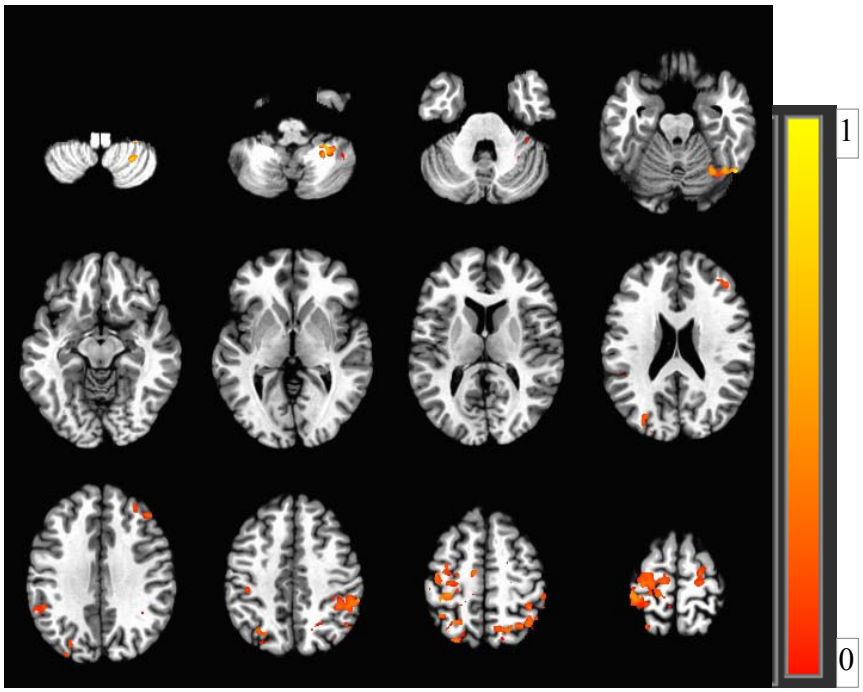

Figure 2-8: Group activation map for "posture" task corrected for p-value of 0.05 and clustered with size of 20 voxels.

From the activation maps for both "posture" and "spiral" tasks, it shows motor areas of the brain (Brodmann Area 4) are activated which was predictable. Visual cortex activation is another point of interest with more strength on spiral drawing task which needs more functionality rather than postural task. The main observation here is the different pattern of activity observed in "posture" and "spiral" tasks which brings the hypothesis that different mechanisms under lied in the brain are responsible for each task.

Table 2-3: Cluster information for group activation map for "posture" task along with percent signal change on individual subject.

Cluster #	Atlas Name	x	y	z	Size	S01	S02	S03	S04	S05
1	LPrG & LBA4	+28.5	+25.5	+65.5	171	0.085	0.6904	0.1557	0.5693	0.4522
2	RIPL	-46.5	+58.5	+44.5	150	0.1610	0.2178	0.2262	0.5770	0.8955
3	LPOCG	+37.5	+34.5	+53.5	77	0.3869	0.7720	-0.0504	0.4563	0.5170
4	LMEFG	+4.5	-31.5	+38.5	58	-0.0573	-0.2975	-0.1953	-0.3434	-0.3253
5	RCT	-28.5	+34.5	-45.5	57	1.9877	0.6427	1.62009	1.6754	1.0161
6	RPRCG	-25.5	+13.5	+65.5	39	0.3262	0.2277	0.3532	0.1039	0.1838
7	RMIFG	-31.5	-40.5	+35.5	37	0.3070	0.1709	0.4841	0.3573	0.1213
8	LIPL	+52.5	+40.5	+23.5	28	11.21	0.6102	0.4584	0.6438	0.20756
9	LSPL	+22.5	+67.5	+44.5	28	0.0276	0.3712	0.2084	0.5460	0.6057
10	LPRE	+25.5	+79.5	+29.5	26	0.0494	0.6273	0.3064	0.1076	0.3919
11	RDEC	-49.5	+58.5	-18.5	21	0.73	0.9153	0.084	0.9007	1.968
12	LBA3	+37.5	+28.5	+53.5	21	0.0979	0.5607	0.2335	0.7348	0.2224

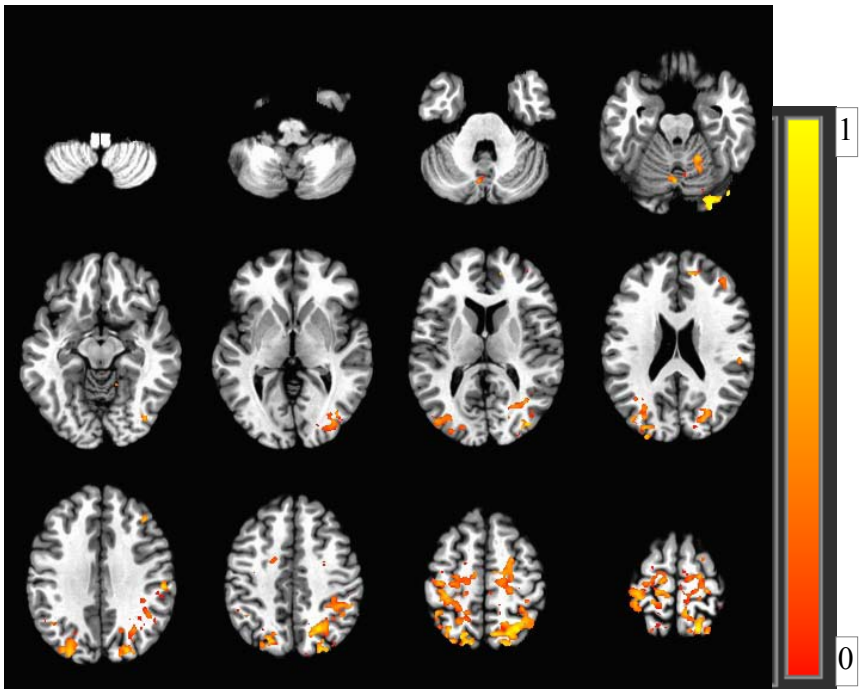

Figure 2-9: Group activation map for "spiral" task corrected for p-value of 0.05 and clustered with size of 20 voxels.

Table 2-4: Cluster information for group activation map for "spiral" task along with percent signal change on individual subject.

Cluster #	Atlas Name	x	y	z	Size	S01	S02	S03	S04	S05
1	RSPL	-22.5	+67.5	+56.5	502	0.7588	1.893	0.3798	0.6463	0.6498
2	LPRE	+10.5	+73.5	+50.5	288	0.0687	0.952	0.526	1.0284	2.0756
3	LPOCG	+28.5	+34.5	+56.5	227	0.4552	1.125	0.4251	0.3813	1.4955
4	RPOCG	-25.5	+28.5	+62.5	132	0.0996	0.9574	1.0433	0.5736	0.3192
5	RIOG	-43.5	+79.5	-15.5	114	0.7382	4.0899	2.9782	1.1772	0.6816
6	RCU	-19.5	+46.5	-15.5	29	0.8411	0.6720	0.5189	0.6328	0.5085
7	LDOV	+1.5	+67.5	-18.5	25	0.8984	0.5371	0.7063	0.9653	0.0641
8	LSTG	+40.5	+58.5	+26.5	25	0.1145	0.2816	0.7532	0.3074	0.2039
9	RPACL	-7.5	+40.5	+56.5	23	0.131	0.6993	0.4505	0.6909	0.1727
10	RMIFG	-40.5	-37.5	+26.5	22	0.5149	0.4854	0.8955	0.6652	0.5890
11	RMEFG	-13.5	-46.5	+14.5	21	0.8248	0.4891	0.7938	1.1576	0.1989
12	RPOCG	-52.5	+25.5	+32.5	21	0.3506	1.1209	1.1872	0.1725	0.3288
13	LMEFG	+7.5	+13.5	+50.5	21	0.4345	0.5776	0.1463	0.3098	0.8818
14	LPRCG	+13.5	+28.5	+62.5	20	0.1460	0.9940	0.5683	0.873	0.4341

Contra lateral activation in motor area, ipsilateral cerebral activity and sensory areas are of our interest. The percent change in BOLD signal verifies the current observations while obviously we have inter subjects variability and that brings the issue of "blob" studies. Figure 2-10 shows the BOLD signal measured for a window of 3 by 3 centered at the center of the mass for the first cluster survived from each task.

Region of Interest (ROI) Analysis

From a priori information and expected pattern of activities in the tasks, fourteen different Regions of Interests (ROIs) were defined and created in standard space. Regions of interest include: Left Brodmann Area 4 (LBA4), Right Brodmann Area 4 (RBA4), Left Brodmann Area 17 (LBA17), Right Brodmann Area 17 (RBA17), Left Dentate (LDEN), Right Dentate (RDEN), Olive (OLI), Left Putamen (LPUT), Right Putamen

(RPUT), Left Red Nucleus (LRN), Right Red Nucleus (RRD) and Vermis (VER). Figure 2-11 shows the ROI location in standard space.

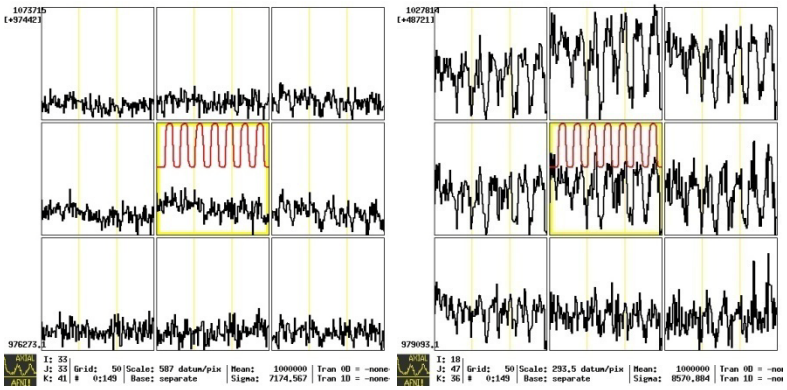

Figure 2-10: BOLD signal measurements at a window centered at the mass of first cluster of "posture" (left) and "spiral" (right) overlaid with experimental paradigm (red time series).

For each region of interest, a mask were made and the average of percent change in BOLD signal for voxels surrounded by the mask were computed in subject basis and the mean value of percent change of BOLD signal for each ROI of each task were finally calculated. Figure 2-12 and 2-13 show percent change in BOLD signal for "posture" and "spiral" tasks across subjects computed in the way explained above. Figure 2-14 is the mean value of percentage change in BOLD signal for each task.

Functional MRI Connectivity Analysis

By connectivity analysis, we are looking for possible hypothesis about the connections among parts in the brain volume. The connectivity could be interpreted as an anatomical connectivity where fibers are involved or it could be neural dependency which made them to work coherently with variable amplitude of correlation. A rich source of connectivity analysis approaches for fMRI could be found in the literature [Beu M et al..

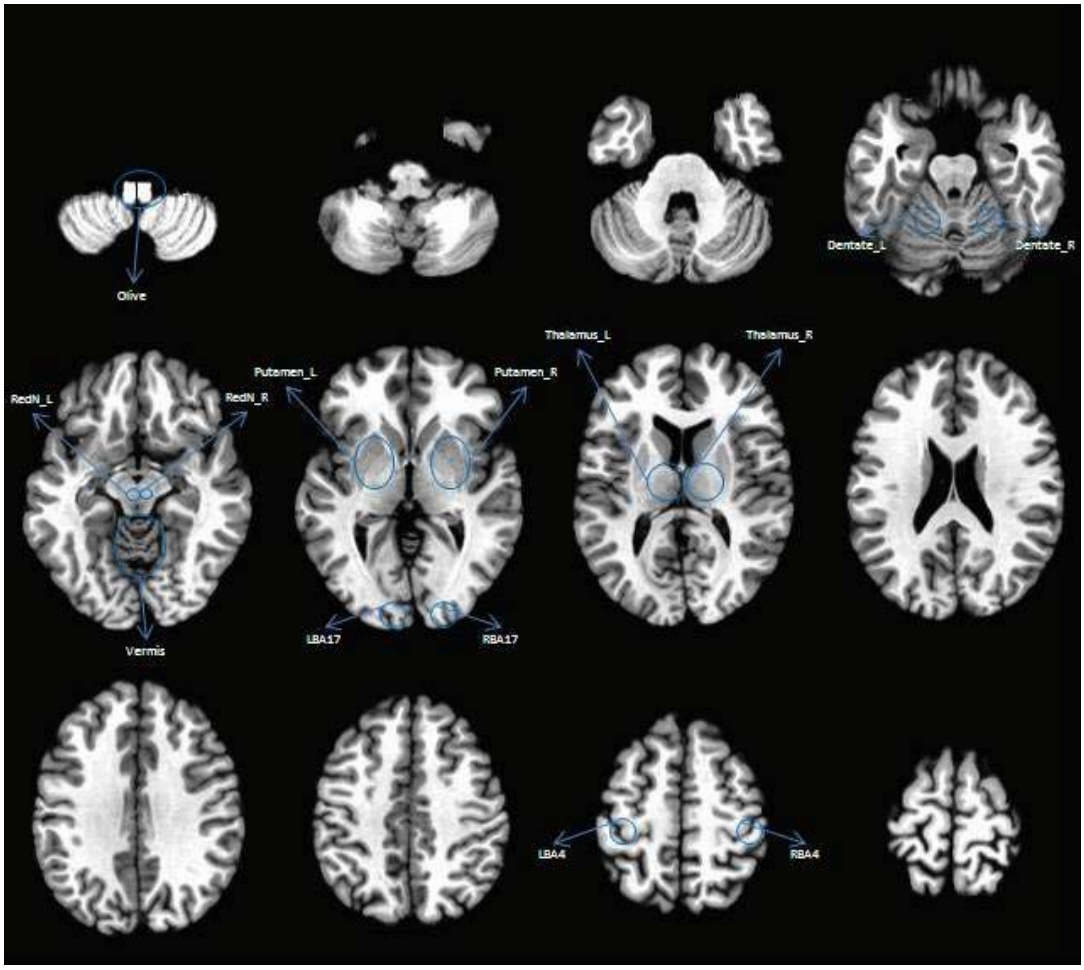

Figure 2-11: Regions of Interest.

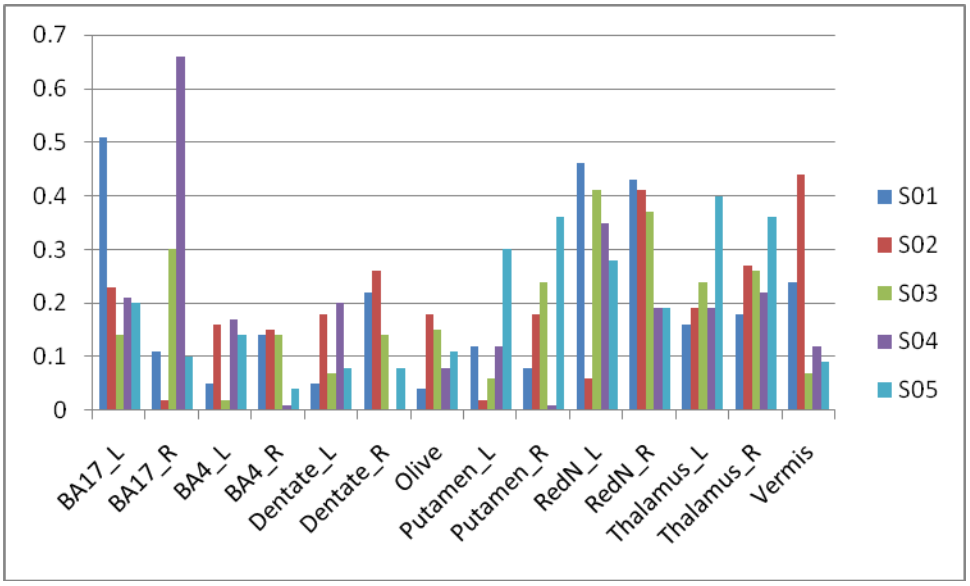

Figure 2-12: BOLD signal percent change in each ROI across subjects for "posture" task.

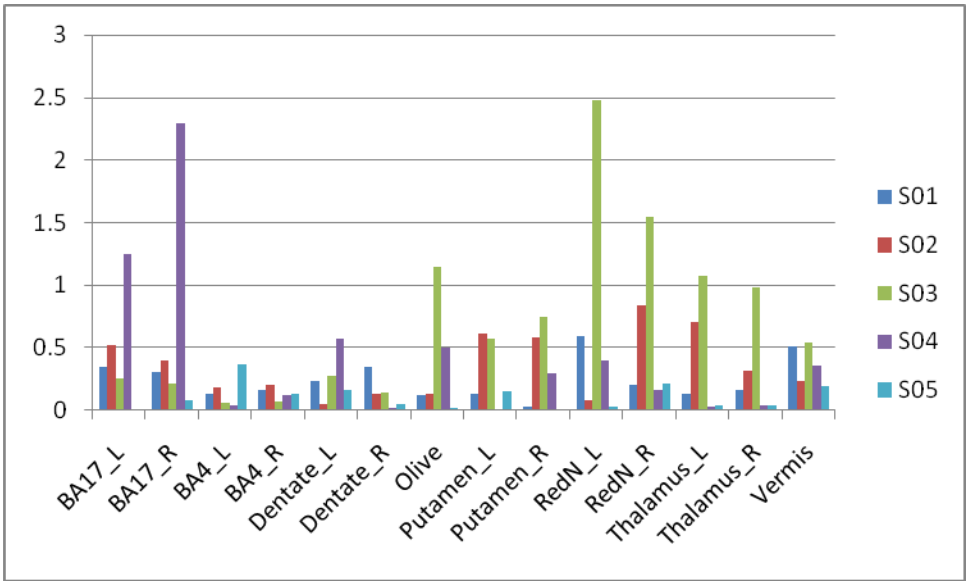

Figure 2-13: BOLD signal percent change in each ROI across subjects for "spiral" task.

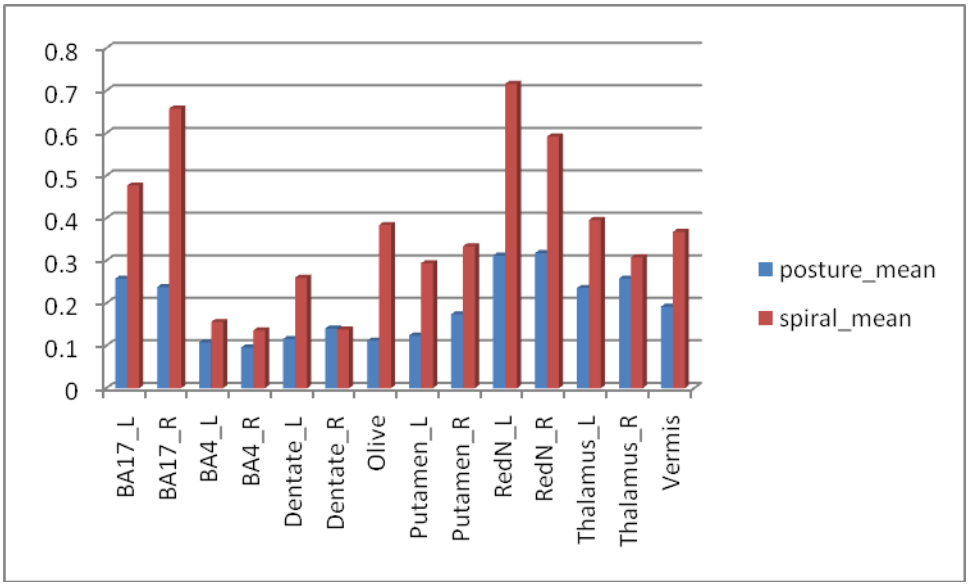

Figure 2-14: Average BOLD signal percentage change in each ROI for "posture" and "spiral" tasks.

2009; De Luca M et al. 2006; Deshpande G et al. 2009; Greicius MD et al. 2009; Lowe MJ et al. 1998; Zang 2004. For fMRI connectivity analysis of ET, we implemented connectivity using seed based global connectivity approach. In this approach, "Seed" region either could be anatomically defined from a standard template using a priori information about the brain networks involved subsequently mapped to the individual

subject brain or from clusters identified in statistical parametric mapping. We chose the first strategy like we defined our regions of interest. The approach works on computing the correlation coefficient between anatomically defined ROI time series and time series extracted from all other parts of the brain. Reference seed time series for each ROI is the average preprocessed time series of all voxels located on the region of interest.

For each seed, a statistical activation map were computed using GLM approach including square of correlation coefficient values which needs to be converted to the correlation coefficient by taking the square root and paying attention to its sign from the estimated β value. To run a group analysis, the correlation coefficient (r) were transformed to Z-scores (z) using Fisher's transformation to have a distribution closer to normal:

$$z = \frac{1}{2}\ln\left(\frac{1+r}{1-r}\right) \qquad (2\text{-}10)$$

Group analyses (ANOVA with mixed factor effects) were applied on the resulted z scores for each ROI. Table 2-5 and 2-6 summarize connectivity maps for each ROI for "posture" and "spiral" tasks by providing which clusters are significantly more likely to be connected to each ROI.

As the tables implies, we observe different connectivity pattern for "posture" and "spiral" tasks while we hypothesize that a network of motor cortex, sensory motor area, visual cortex, cerebellum are involved in both. Both contra and ipsilateral Thalamic areas are shown to be active in the defined network

Table 2-5: Seed based Connectivity analysis of functional MRI in "posture" task.

BA17_L	LLG; LBA17; LPRE; RPRCG; LPOCG; RSPL; LMEFG
BA17_R	RLG; RBA17; LPRE; LPOCG; LMeFG; RISLL; RPRCG; RIPL; RPRE; RMeFG
BA4_L	LPOCG; RIFG; LPRCG; LBA44
BA4_R	RPRCG; RBA6; RBA4; LMIFG; LCT; LSTG; LBA22
Dentate_L	LCUL; LDEC; LSFG; LCUN; RPOCG; RPRE;
Dentate_R	RCUL; RDEC; LMEFG; RPC; RIPL; LPRCG; LPC; RPACL;
Olive	RBS
Putamen_L	LLEN; LPUT; LMeFG; LBA6; RCLA; RPRE; RBA31; LPRE; RPOCG; RBA40;
Putamen_R	LDEC; RLEN; RPUT; RMEFG; LCG; LSFG
RedN_L	LTHA; LREDN
RedN_R	LCG; RT; RREDN; RPAHG;
Thalamus_L	LTHA; MABO; RPACL; RBA31; LINS; RCLA; LMEFG;
Thalamus_R	RTHA; RMEDN; RPRE; RBA7; RINS; LMEFG;
Vermis	LCOV; LMIFG;LBA10; LMITG

Table 2-6: Seed based Connectivity analysis of functional MRI in "spiral" task.

BA17_L	LLG; LBA17; LSPL;RSPL;RBA17; RPRE; RCT;
BA17_R	RCUL; RBA17; RMIOG; LDEN;
BA4_L	LPoCG; LBA4; RMIFG; LFUG;
BA4_R	RPRCG; RBA4; LSOG; RINS; RBA13; LPRCG; LMIFG; RMIFG; RPOCG;
Dentate_L	LCUN; LDEC; RPC; RBA30; LMEFG; RSTG; LCLA; LPUT; RPRCG; RBA4;
Dentate_R	RCUN; RDEC; RMIFG; LCLA; LPUT; RSFG; RBA9;
Olive	RBS;
Putamen_L	LMEFG; LLEN; LPUT; RCAU; LMITG; RPC;
Putamen_R	RINS; LMEFG; RLEN; RPUT;
RedN_L	N/A
RedN_R	N/A
Thalamus_L	LPC; LPACL; LBA31; LTHA; LAN; LIPL; LMITG; RIPL; RVLN; RPRCG; LPRE; LIPL; LBA40;
Thalamus_R	RPAHG; RTHA; RMEDN; LPRCG; RPRE; RPRCG; LMITG; RCUL
Vermis	RDEC; RPRE; RIPL;

Summary of Findings

This chapter explained an overview of what functional Magnetic Resonance Imaging could provide us on brain activation. The experimental setup to assess the brain activity and networks involved in Essential Tremor and more specifically kinetic and postural tremor introduced. Statistical activation mapping showed different brain regions are involved in introducing kinetic and postural tremor. Regions of Interests analysis verified the observation of activation mapping where there were statistically significant changes in BOLD-fMRI percent signal change for regions involved for kinetic tremor with more strength on visual cortex. Global connectivity of the brain were implemented by employing seed and target based correlation analysis methodology.

Chapter 3. Objective Measurement of Tremor of Essential Tremor

While there is no definite cure for Essential Tremor (ET), there are treatments reported successfully applicable to some patients. Early diagnosis of ET like most other diseases could increase the chance of being treated properly. Nowadays, Essential Tremor is best diagnosed by an experienced physicist in clinics specialized to movement disorders. Along with the patient description of their experience of tremor and challenges they have in daily activities plus medical history and family history, there are inclusion and exclusion criteria for the probable ET diagnosis such as the tremor location, mechanism of tremor generation including the type of activities introducing tremor (postural and kinetic) and the muscles involved during tremor (extensor and flexor muscles simultaneously are under stress in ET), life time of tremor.

Clinical assessment of essential tremor are being handled through rating scales such as Washington heights-Inwood Genetic Study of Essential Tremor (WHIGET) tremor rating scale or more objectively by drawing spirals and handwriting in kinetic tremor severity measurement and pouring water in postural tremor severity test. The more shaky handwriting or the more spilled water out of the glass the more severe situation of tremor we face. It yet lacks a systematic way of assessing tremor acerbity in a sense that the results of both tests are evaluated visually and subjective to the clinician perception of the symptoms and introducing variability. Analyzing EMG recordings, spirogram and acceleration proposes a new set of measurements to quantify severity using time and frequency investigation of recordings [Mansur PH et al. 2007; Elble RJ et al. 1996; Elble RJ et al. 1990; Heldman DA et al. 2011; O'Suilleabhain et al. 2001; Bacher M et al. 1989].

This chapter is on the analysis of Accelerometry and Spirography recordings in our experiments. First the accelerometer is introduced and our processing steps to extract information were explained. The spirography is discussed next and the results will be followed.

Accelerometry Data Recording

Accelerometry data were recorded during the "posture" task where the subject is being instructed to elevate the right arm into a fixed position to fight the gravity. Figure 3-1 shows our accelerometer recording system.

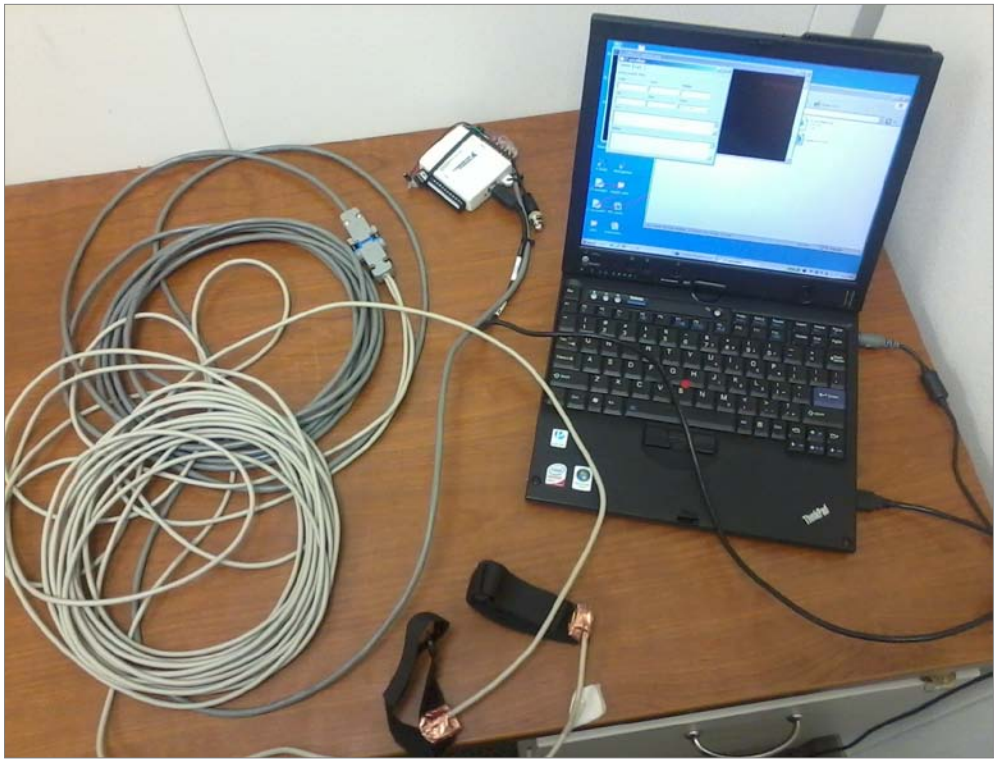

Figure 3-1: Accelerometry recording Facilities.

The whole system is divided into two main parts: The part with functionality inside MR scan room and the part located outside the MR room. The connection between the inside and outside part is through a pair of DB-9S connectors. The inside part includes:

Accelerometer sensors which are Triple-axis accelerometers with three analog output in X, Y and Z direction from the Analog Devices, Inc. (ADI) is responsible to measure the acceleration and convert it to an output signal. The sensing mass is connected with a spring in conjunction with a damper to damp the spring motions. The second law of motion (Newton) is the base of working accelerometer which proposes that the electromotive force (net force includes acceleration induced force, damper induced force and spring induced force) applied to the mass has linear relation with the accelerometer measured in direction of the mass moving. The sensor implements a MEMS technology in conjunction with differential capacitive position sensing to meter the acceleration. They are attached to black belts to fix them on the dorsal area of the subject's hand. **White cable** to transfer the analog recordings from the sensor to the connection point where the outside part starts with **gray cable** is responsible to deliver the recordings to a **multifunction I/O device**, NI USB-6008 with 8 analog inputs, 2 analog inputs and 12 digital I/O, to convert to the digital pulses and finally save them in the working machine (lenova thinkpad x61) to record the digital data.

Spirography Data Recording

Circular spirography were directed during the spiral task represented by "kinetic" symbol to characterize the kinetic tremor which occurs during voluntary movements. The setup to record the Archimedes spiral is shown in Figure 3-2. The spiral recording process is to record the horizontal (X) and Vertical (Y) coordinates of the points on the MR compatible resistive tablet where they were touched by the non marking pen during spiral drawing by the subject. The spiral recordings travel trough the same route as accelerometer data before recorded by the machine.

Figure 3-2: Spiral recording setup.

Accelerometry and Spirography Data Analysis

As it was pointed out before, Accelerometry measures the accelerations along three axes and Spirography measures the displacement along two axes. The following is our proposed pipeline to assess the tremor power which is likely to indicate the severity of tremor. We implemented the quantitative processing of recorded data in python programming language.

Low Pass Filtering

First we apply a low pass filter by implementing one of the most common Finite Impulse Response (FIR) filters, moving average filter, to attenuate the random noise in the digital signal by averaging the high frequency noise. A window size of 10 assures to preserve the frequency components which are likely to be tremor dependent. The moving average

window was sliding over each individual channel and the outputted signals were forwarded to the next block to evaluate the frequency spectral.

Spectral Analysis

One interesting characteristic of ET is the observation of dominant frequency components related to the tremor in frequency domain analysis of the recordings. Spectral analysis was done by implementing a Fast Fourier Transform (FFT) technique [Mansur PH et al. 2007]. The input is the channel in time domain and the output is a complex array. The power is computed by taking the absolute values of the output array for each corresponding frequency component. Equations (3-1) and (3-2) provides the Fourier Transform (FT) of a discrete signal and power spectrum of the correspondence respectively.

$$X[k] = \sum_{n=0}^{N-1} x[n] e^{-2\pi kn / N} \tag{3-1}$$

$$P[k] = \left| X(k) \right|^2 \tag{3-2}$$

Where $x[n]$ is the signal in the time domain and $X[k]$ is the corresponding frequency domain representation of signal. Figures 3-3 and 3-4 are the accelerometry and spirography data recordings in time and frequency domain for each individual channel.

Tremor Quantifying

This step is implemented through a couple of steps: first tremor powers and respective frequencies were extracted for each channel (X, Y, Z for accelerometry; X and Y for Spirography). This was done by finding the dominant power in frequency domain and looking up the frequency corresponding to that power value. To have a single value presenting the tremor power we defined the followings:

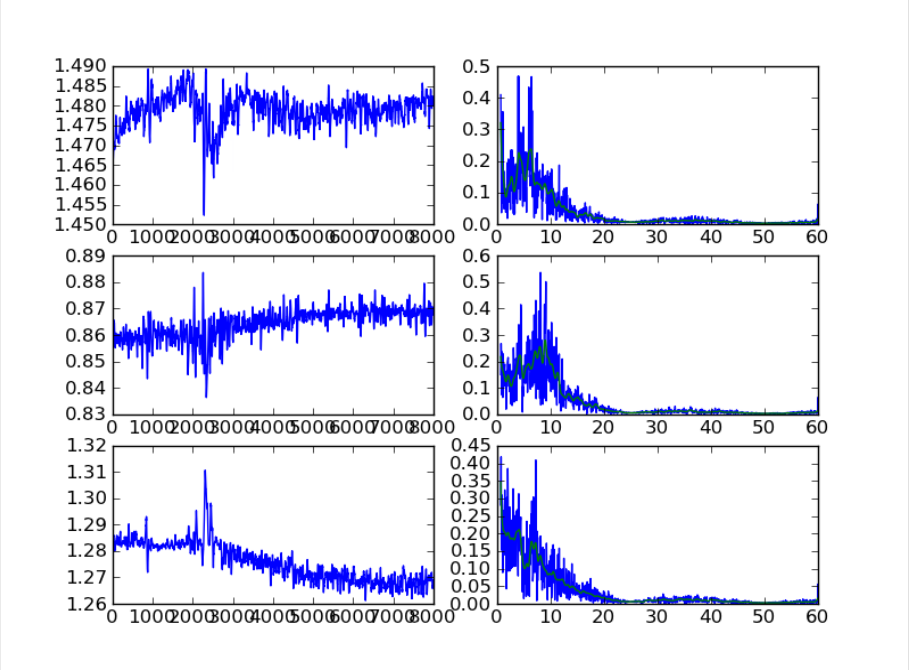

Figure 3-3: Accelerometry Data Recording (rows: X, Y, Z channels) in Time (First column) and Frequency (Second column).

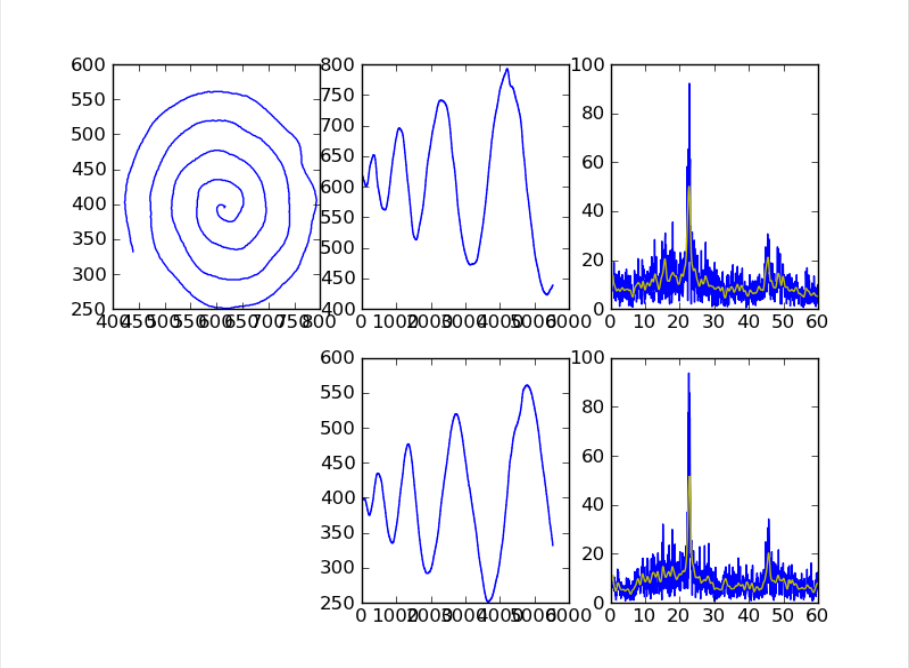

Figure 3-4: Spirography Data recording. Spiral Drawn (top left), displacement measurement in X and Y (middle column), Frequency power spectrum (third column).

Net Tremor Frequency

Weighted average of tremor frequencies of individual channels computed through equation (3-4).

$$f_T = \frac{1}{\sum_{n=1}^{N_{ch}} P_n} \sum_{n=1}^{N_{ch}} P_n f_n \tag{3-3}$$

Net Tremor Power

Euclidean norm of the vector containing the tremor powers from different channel calculated using equation (3-5).

$$p_T = \sqrt{P_1^2 + P_2^2 + \ldots + P_{N_{ch}}^2} \tag{3-3}$$

Net Tremor Frequency and Power Measurements

Table 3-1 and 3-2 include the computed tremor frequency and power across subjects. Computed tremor frequencies falls in the range of 2 to 8 Hz. Postural tremor powers are normalized to the kinetic tremor power.

Table 3-1: Tremor frequency (Hz) and power computed from the proposed pipeline across subjects using accelerometry recording.

	Frequency (Hz)	power
S01	6.441	202.597
S02	5.86	1696.926
S03	2.602	116.317
S04	6.029	3664.617
S05	7.363	660.7411

Table 3-2: Tremor frequency (Hz) and power computed from the proposed pipeline across subjects using spirography recording.

	Frequency (Hz)	Tremor power
S01	3.148	264.2
S02	5.063	1088
S03	3.521	281.5
S04	6.087	3914
S05	4.972	793.5

Figures 3-5 and 3-6 show the tremor frequency and tremor power measured using two different modalities (accelerometry and spirography). As the figure implies and by visually inspection of the above tables, the measured tremor power from postural task and from kinetic task (spiral) look to co vary linearly but this is not the case for postural and kinetic tremor frequencies.

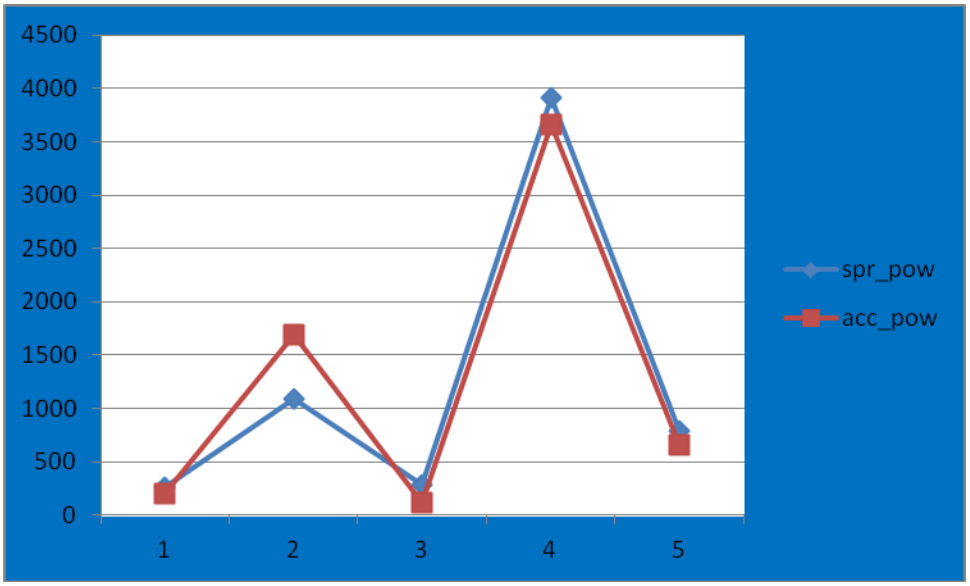

Figure 3-5: Net Tremor power of kinetic (spiral drawing) and postural (accelerometry) tasks.

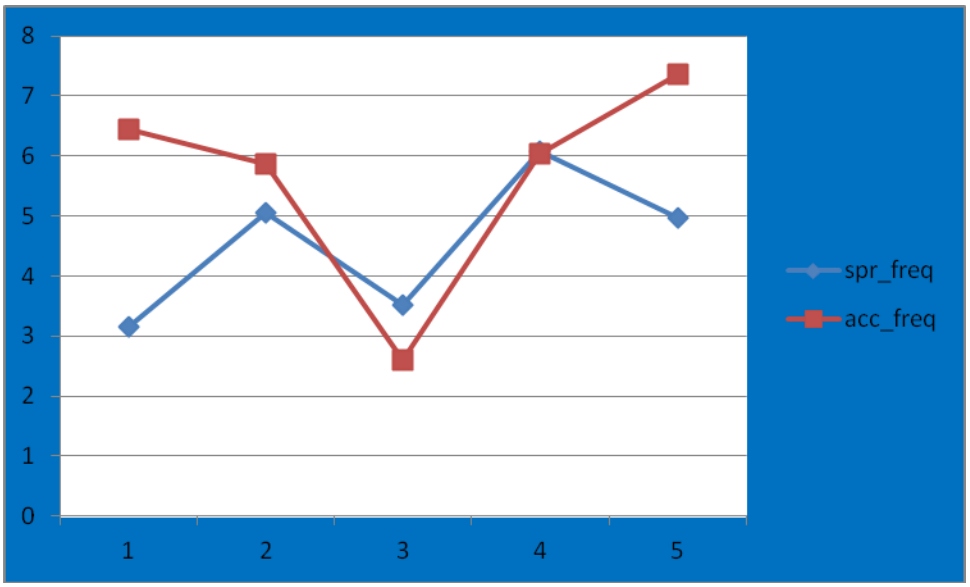

Figure 3-6: Net Tremor frequency of kinetic (spiral drawing) and postural (accelerometry) tasks.

The difference observed in the computed tremor frequency of postural and kinetic tremor may be due to the different oscillatory network involved in the brain.

Summary of Findings

This chapter explained two objective measurements of tremor during postural and kinetic tremor appearance. An analysis pipeline was proposed to assess the tremor severity by defining a net tremor frequency and net tremor power. Different net tremor frequency observed during postural and kinetic tremor hypothesized the existence of different oscillators to generate each tremor in the brain.

Chapter 4. A Conjunction Study

After characterizing the kinetic and postural tremor by analysis of functional MRI and consecutively measuring the tremor power and frequency by the hands of objective tools (Accelerometry and Spirography Recording) during the execution of "posture" and "spiral" tasks, we are now willing to go one step further. The question we are interested at this point is whether there is a relationship between the objective measurement and fMRI study. More clearly, could we predict the tremor state of severity (e.g. by providing a level of tremor power) using measurements of functional MRI.

We employed the Ordinary Least Square Regression (OLSR) model which we introduced in chapter 2 to find the relationship between fMRI measurements and tremor power measured by accelerometry and spirography. We defined a linear model for our analysis expressed in terms of the regions of interest (ROI) fMRI-BOLD signal measurements and output of the model is to be the tremor power as it is shown in equation (5-1).

$$P_t = \alpha + \beta_{BA17\_L} B_{BA17\_L} + \beta_{BA17\_R} B_{BA17\_R} + \beta_{BA4\_L} B_{BA4\_L} + \ldots + \beta_{Vermis} B_{Vermis} + \varepsilon \tag{5-1}$$

Where P_t is the tremor power, $B_{(.)}$ is the fMRI BOLD signal measurements on ROI and the $\beta_{(.)}$ are the parameter models needed to be estimated from the regression analysis. Least square regression estimates the model parameters by minimizing the sum of squared error defined by equation (5-2) and yields the parameter in equation (5-3) as an example for one of ROI's.

$$SSE = \sum_{i=1}^{14} e_i^2 \tag{5-2}$$

Due to the small number of training dataset we had, a selection methodology was implemented in advance to running the regression. To choose among the Regions of Interests, we choose the ones who explains more of the variance occurred in tremor

power due to each individual fMRI-BOLD signal measurement of each ROI. It is worth to recall that BOLD measurement for each ROI is the average percent change in BOLD signal measured during fMRI experiment. Figures 5-1 and 5-2 show the explained variance in tremor power by each ROI when individually incorporated the regression model in equation 5-1 without having other ROI measurements joined.

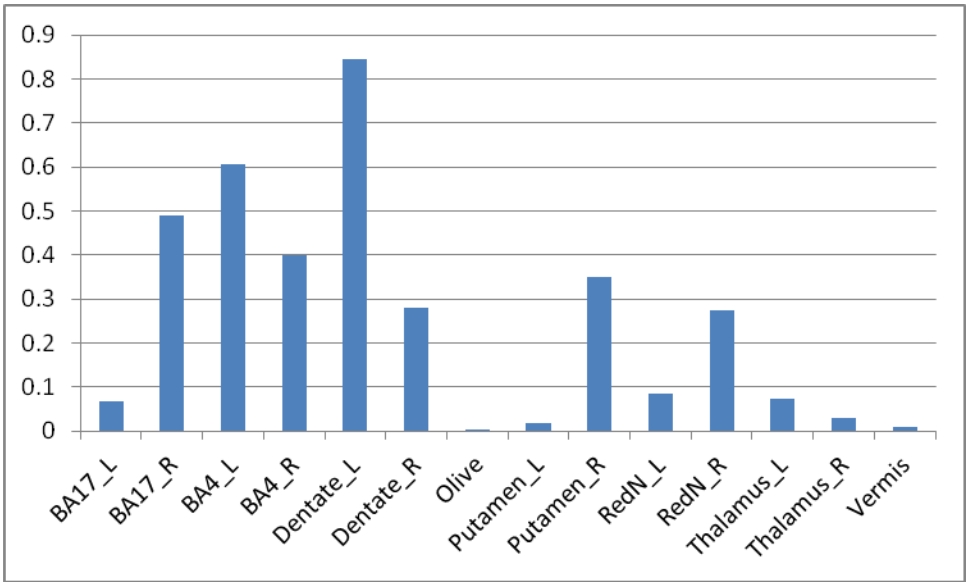

Figure 4-1: Explained variance of tremor power by each individual ROI fMRI BOLD signal percent change during postural task.

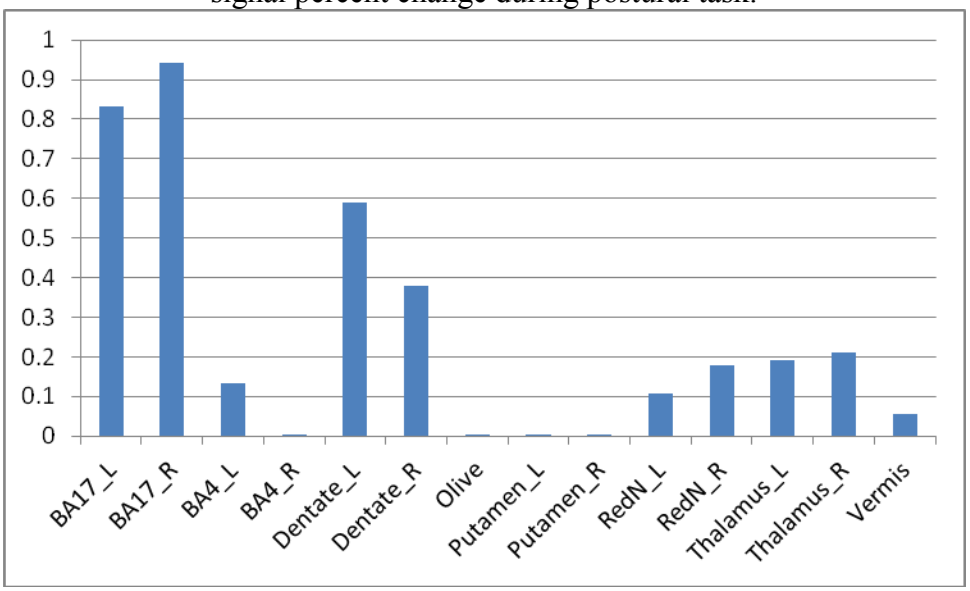

Figure 4-2: Explained variance of tremor power by each individual ROI fMRI BOLD signal percent change during spiral task.

Ranking the parameters give us the indication of including BA17_L, BA17_R, BA4_L, BA4_R, Dentate_L, Dentate_R, Putamen_L and Thalamus_L in our model and exclude the remaining. Running the regression analysis, we found the given model in equation 5-3 explains %98 of the variance observed in tremor power.

$$T = 2498.1B_{BA17\_L} + 6460.5B_{BA17\_R} + 26735B_{BA4\_L} - 21508B_{BA4\_R} - 18492B_{Dentate\_L} + 13827B_{Dentate\_R} - 18530B_{Putamen\_L} + 13332B_{Thalamus\_L} - 2368 \quad (5\text{-}3)$$

Summary of Findings

A linear model was defined to predict the tremor severity (power) using functional MRI measurements. Parameters of the model were defined through a ranking technique proposed and the least square regression analysis estimated the model parameters which best fit the model. Proposed model explained %98 of the output variance.

Chapter 5. Conclusion and Future Works

Postural tremor and Kinetic tremor were introduced and their characteristics are objectively assessed using functional magnetic resonance imaging technique in conjunction with quantifying the tremor severity. A pipeline to analyze the acquired fMRI BOLD signals were proposed. The pipeline first tries to increase the Signal to Noise (SNR) ratio by reducing the unwanted variances to signify the variances of interest with available understanding of fMRI signal. Activated regions were statistically identified. Postural and kinetic tremor s showed different pattern of activities. Using a priori information on Essential Tremor characteristics, regions of interest analysis were directed to study the percent change in BOLD signal. Seed based connectivity analysis to define a hypothesis on networks in Essential Tremor were done showing the motor area, thalamic area, sensory area and cerebellum explaining most of the variance in ET related brain activity.

Two conventional techniques to objectively measure the tremor characteristics were used to evaluate the disease state. A processing pipeline to gain the tremor severity and frequency analysis of kinetic and postural tremor were proposed. The proposed method resulted in different pattern of frequency range in postural and kinetic tremor.

A conjunction study were done to propose a model to connect the fMRI finding and measurements from accelerometry and spirography and find the covariance behavior. The proposed model after training phase gives the tremor power (severity) by measuring BOLD-fMRI signals across the network considered in our model.

The dataset we employed in the thesis included the measurements of the same subjects repeating the same experiments with having one serve of Ethanol to study the effect on

tremor suppression. Figure 5-1 and 5-2 shows the group activation maps before and after taking the medication for postural and spiral task respectively.

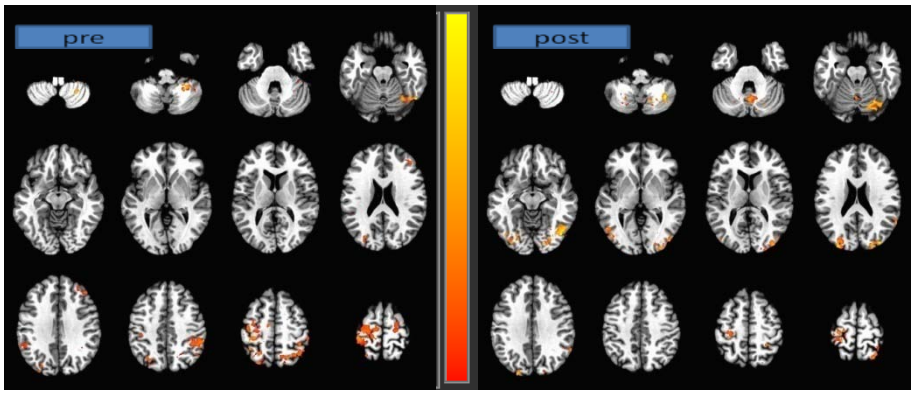

Figure 5-1: Group activation maps for postural task pre and post taking the medication.

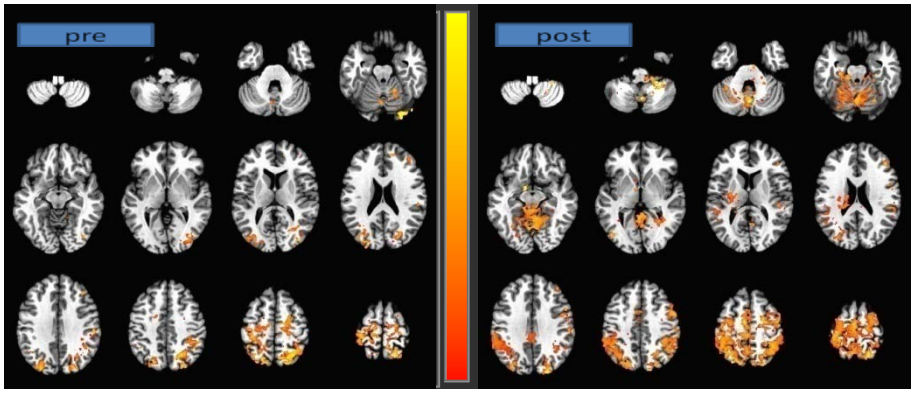

Figure 5-2: Group activation maps for spiral task pre and post taking the medication.

Observing the different response to Ethanol for postural and kinetic tremor is of interest. Figure 5-3 and 5-4 shows how ethanol affects the tremor power and frequency in a subject. As the figures imply the tremor power significantly reduced after taking the medication. Also tremor frequency (dominant component in frequency domain) shifted to lower frequency. For the entire hypothesis, more subjects are needed to be recruited as future work.

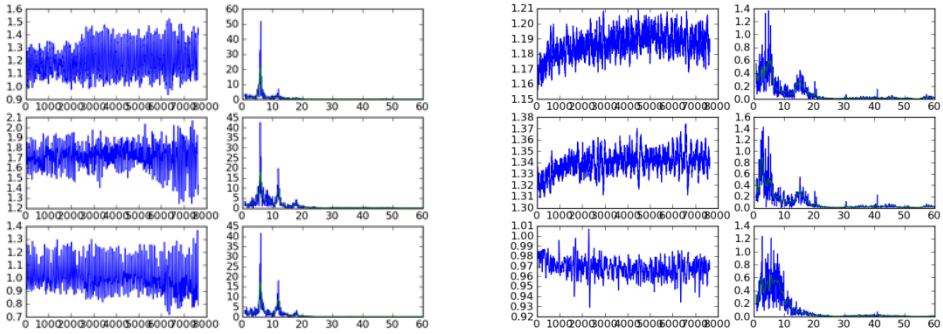

Figure 5-3: Accelerometry data analysis during the postural task for pre- and post taking medication.

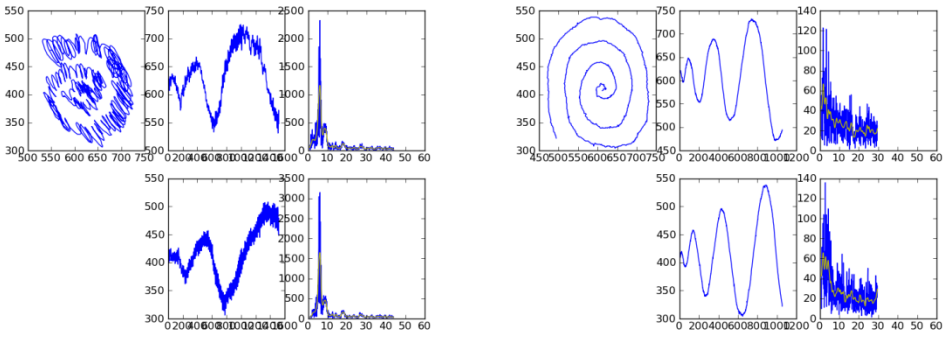

Figure 5-4: Spirography Data analysis for spiral task for pre- and post taking medication.

Our first observation on postural and kinetic tremor frequency were the distinction among them which could be a result of different oscillators involved. Student test could not provide any significant difference between the mean of frequencies for postural and kinetic tremor. More subjects are needed to accurately comment on this issue.

In connectivity analysis of fMRI data, we defined global connectivity networks for kinetic and postural tremor but there is no causality involved in the network. Structural Equation Modeling (SEM) showed to be an approach to aim causal networks in fMRI where we look for effective connectivity as future work.

Works Cited

Abdo WF, van de Warrenburg BP, Burn DJ, Quinn NP, Bloem BR. The clinical approach to movement disorders. Nat Rev Neurol. 2010; 6(1):29-37.

Anderson JS, Dhatt HS, Ferguson MA, Lopez-Larson M, Schrock LE, House PA, Yurgelun-Todd D. Functional connectivity targeting for deep brain stimulation in essential tremor. AJNR Am J Neuroradiol, 2011; 32(10):1963-8.

Bacher M, Scholz E, Diener HC. 24 hour continuous tremor quantification based on EMG recording. Electroencephalogr Clin Neurophysiol. 1989; 72(2):176-83.

Beu M, Baudrexel S, Hautzel H, Antke C, Mueller HW, Neuraltraffic as voxel-based measure of cerebral functional connectivity in fMRI. J Neurosci Methods.2009;176(2):263-9.

Blomstedt P, Lindvall P, linder J, Olivecrona M, Forsqren L, Hariz Ml. reoperation after failed deep brain stimulation for essential tremor. World neurosurg. 2012.

Boecker H, Wills AJ, Ceballos-Baumann A, Samuel M, Thompson PD, Findley LJ, Brooks DJ. The effect of ethanol on alchol-responsive essential tremor: a positron emission tomography study. Ann Neurol. 1996;39(5):650-8.

Boller F and Grafman J. Handbook of neuropsychology. 1994; 9. Elsevier Science Publishers B.V. Breit S, Spieker S, Schulz JB, Gasser T. Long-rterm EMG recordings differentiate between parkinsonian and essential tremor. J Neurol 2008;255(1):103-11.

Bucher SF, Seelos KC, Dodel RC, Reiser M, Ortel WH. Activation mapping in essential tremor with functional magnetic resonance imaging. Ann Neurol 1998,43(3):410.

Cox RW. AFNI: software for analysis and visualization of functional magnetic resonance neuroimages. Comput Biomed Res. 1996; 29(3):162-73.

Cox RW. AFNI: What a long strange trip it's been. Neuroimage. 2011.

Dale Am, Fischl B, Sereno Ml. Cortical surface-based analysis. I. Segmentation and surface reconstruction. Neuroimage. 1999;9(2):179-94.

De Luca M, Smith S, De Stefano N, Federico A, Matthews PM. Blood oxygenation level dependent contrast resting state networks are relevant to functional activity in the neocortical sensorimotor system. Exp Brain res. 2005;167(4):587-94.

Deng H, Le W, Jankovic J. Genetics of essential tremor. Brain. 2007; 130(6):1456-64.
Deshpande G, LaConte S, Peltier S, Hu X. Integrated local correlation: a new measure of local coherence in fMRI data. Hum Brain Mapp. 2009;30(1):13-23.

Deuschl G, Bain P, Brin M. Consensus statement of the movements disorder society on tremor. Ad hoc scientific committee. Mov Disord. 1998;13(3):2-23.

Elble RJ, Brilliant M, Leffler K, Higgins C. Quantification of essential tremor in writing and drawing. Mov Disord. 1996; 11(1):70-8.

Elble RJ, Sinha R, Higgins C. Quantification of tremor with a digitizing tablet. J Neurosci Methods. 1990;32(3):193-8.

Feys P, Helsen W, Prinsmel A, Ilsbroukx S, Wang S, Liu X. Digitised spirography as an evaluation tool for intention tremor in multiple sclerosis. J Neurosci Methods. 2007;160(2):309-16.

Fischl B, Sereno Ml, Dale AM. Cortical surface-based analysis. II: Inflation, flattening, and a surface-based coordinate system. Neuroimage 1999;9(2):195-207.

Friston KJ, Holmes AP, Poline JB, Grasby PJ, Williams SC, Frackowiak RS, Turner R. Analysis of fMRI time-series revisited. Neuroimaging Clin N Am. 1995;5(2):207-25.

Greicius MD, Supekar K, Menon V, Dougherty RF. Resting-state functional connectivity reflects structural connectivity in the default mode network. Cereb Cortex. 2009;19(1):72-8.

Heldman DA, Jankovic J, Vaillancourt DE, Prodehl J, Elble RJ, Giuffrida JP. Essential tremor quantification during activities of daily living. Parkinsonism Relat Disord. 2011;17(7):537-42.

Hellwig B, Haubler S, Schelter B, Lauk M, Guschlbauer B, Timmer J, Lucking CH. Tremor-correlated cortical activity in essential tremor. THE LANCET. 2001; 357: 519-23.

Hellwig B, Schelter B, Guschlbauer B, Timmer J, Lucking CH. Dynamic synchronization of central oscillators in essential tremor. Clin Neurophysiol 2003;114(8): 1462-7.

Hua S, reich SG, Zirh AT, Perry V, Dougherty PM, Lenz FA. The role of the thalamus and basal gangalia in parkinsonian tremor. Mov Disord. 1998; 13(3):40-2.

Khan AR, Wang L, Beg MF, FreeSurfer-initiated fully-automated subcortical brain segmentation in MRI using large deformation diffeomorphic metric mapping. Neuroimage.2008;41(3):735-46.

Kim B, Boes JL, Bland PH, Chenevert TL, Meyer CR. Motion correction in fMRI via registration of individual slices into an anatomical volume. Magn Reson Med. 1999; 41(5):964-72.

Kondziolka D, Ong JG, Lee JY, moore RY, Flickinger JC, Lunsford LD. J. Gamma knife thalamotomy for essential tremor. Neurosurg. 2008; 108(1):111-7.

Logothetis NK. The neural basis of the blood-oxygen-level- dependent functional magnetic resonance imaging. Philos Trans R Soc Lond B Biol Sci. 2002:357(1424):1003-37.

Louis ED. Treatment of Essential Tremor: Are there issues we are overlooking?. Front Neurol. 2012; 2:91.

Lowe MJ, Mock BJ, Sorenson JA. Functional connectivity in single and multislice echoplanar imaging using resting-state fluctuations. Neuroimage.1998;7(2):119-32.

Mansur PH, Cury LK, Andrade AO, Pereira AA, Miotto GA, Soares AB, Naves EL. A review on techniques for tremor recording and quantification. Crit Rev Biomed Eng. 2007; 35(5):343-62.

Moghal S, Rajput AH, D'Arcy C, Rajput R. Prevalence of movement disorders in elderly community residents. Neuroepidemiology. 1994; 13(4):175-8.

Nahab FB, Peckham E, Hallet M. Essential tremor, deceptively simple ... Pract Neurol. 2007; 7(4):222-233.

Naqvi SA, Ishaq M, Haider QU, Mohammad JS, Ilyas S, Sheikh M. Tremors and its determinants: a 7-years study at a secondary care hospital. J Pak Med Assoc. 2011; 61(9):896-900.

Ogawa S, Lee TM, Kay AR, Tank DW. Brain magnetic resonance imaging with contrast dependent on blood oxygenation. Proc. Natl. Acad. Sci. 1990; 87:9868-72.

O'Suilleabhain PE, Deway RB Jr. Validation for tremor quantification of an electromagnetic tracking device. Mov Disord. 2001;16(2):265-71.

Schenck JF. Safety of strong, static magnetic fields. J Magn Reson Imaging. 2000; 12(1):2-19.

Segonne F, Dale AM, Busa E, Glessner M, Salat D, Hahn HK, Fischl B. A hybrid approach to the skull stripping problem in MRI. 2004; 22(3): 99-113.

Seki M, Matsumoto Y, Ando T, Kobayashi Y, Lijima H, Naqaoka M, Fujie MG. Filtering essential tremor noise on surface EMG based on squared sine wave approximation. Conf Proc IEEE Eng Med Biol Soc. 2011: 7487-91.
Smith SM. Fast robust automated brain extraction. Hum Brain Mapp. 2002; 17(3): 143-55.

Subasi A. Epileptic seizure detection using dynamic wavelet network. Expert Syst. Appl. 2005; 29(2):343-55.

Talairach J, Tournoux P. Co-planar stereotaxic atlas of the human brain: 3-dimensional proportional system- an approach to cerebral imaging. 1988; Thieme Medical Publishers.

Whitcher B, Solutions M, Schmid VJ, Maximilians L. Working with the DICOM and NIfTI data standards in R. Journal of statistical software. 2011; 44(6):1-28.